Final Report

AMERICAN PETROLEUM INSTITUTE
PRAC PROJECT 82-45
RHEOLOGICAL CHARACTERIZATION OF FRACTURING FLUIDS

by

Robert K. Prud'homme
Department of Chemical Engineering
Princeton University
Princeton, New Jersey 08544

OUTLINE

I. INTRODUCTION

This is the final report on our research conducted under the American Petroleum Institute's PRAC Project 82-45 entitled "Rheological Characterization of Fracturing Fluids". The project was initiated by the American Petroleum Institute (API) because: 1) the expense of hydraulic fracturing makes it desirable to understand the process fully, including the rheology of the fracturing fluid, to ensure a successful fracturing operation, and 2) during a round-robin testing program by several laboratories the viscosities reported by the participants for identical gel formulations varied by 1000%.

The purpose of this report to to provide a working guide to rheology of guar gels. We first provide, in Section II, a summary of the significant results and conclusions from the first year of this investigation. In Section III dynamic oscillatory shear measurements, which are used to study guar rheology and guar gel structure, are described. Dynamic oscillatory shear measurements can be directly related to the number of network crosslinks. These measurements and their interpretation are discussed in detail, since they are probably less familiar to researcher in the oil production research area than are steady shear measurements. In Section IV we describe the rheological instruments used in this study. In Section V the preparation of guar samples is detailed. The composition of the model guar gel used in this study was specified by the API Steering Committee. Our observations on the factors controlling gel rheology, including chemical effects, sample preparation effects, and flow history effects are presented in Section VI. In Section VII a model that describes the rheology of gelling fluids is described. The model is based on the temporary network theories used to describe the rheology of polymer melts and solutions. To this theory we have incorporated the chemical kinetics of metal ion adsorption onto the guar polymer backbone and subsequent polymer-polymer crosslinking. In the final sections recommendations for rheological instrumentation and for future research are presented.

At the quarterly meetings with the API Committee overseeing this work several hundred pages of experimental data were distributed. All of that data are not included in this report. Rather the important conclusions drawn from those data are presented along with the relevant data that support those conclusions. The original data are on file with the API publications department and can be obtained through the API.

II. SUMMARY OF CONCLUSIONS

Dynamic oscillatory and steady shear measurements have been used to study the rheology of guar gels. Dynamic oscillatory measurements have been used to study the slow hydration of guar polymer and the effects of chemical composition and mixing on guar gel structure. Steady shear measurements have been used to simulate process conditions. Major conclusions, presented in the body of this report, include the following:

- Results from polymer kinetic theory can be used to relate the measured storage modulus, G', to the crosslink density in the guar gel.

- Aged titanate solutions produce gels with lower values of G'; and therefore, dynamic oscillatory measurements can be used to quantify titanate reactivity.

- Adding diketone (that is, acetylacetone) to modify the rate of reaction does not just slow down the reaction, but it also prevents the gel from crosslinking to the same extent at room temperature as gels without added acetylacetone.

- Mixing is shown to play a crucial role in the development of gel structure. Poor mixing appears to produce microscopically inhomogeneous gel networks that have higher levels of elasticity than homogeneous gels.

- To produce intimately mixed fluids we have developed a novel impingement mixing device.

- Measurements of the steady shear viscosity of gels indicate that wall slip is occurring. However, conventional rheological techniques for calculating wall slip velocities have given contradictory results. There is a need for direct measurements of velocity fields in shear flow to clarify the mechanism of wall slip. In the next year we will be conducting laser doppler measurements to address this problem.

- Under quiescent conditions dynamic oscillatory measurements show that the guar continues to crosslink over a time scale of about 15 minutes. The steady shear measurements show that shear increases the rate of reaction.

- A novel network theory coupled with chemical reaction kinetics is proposed; material functions can be expressed analytically. This model provides a framework for modeling and predicting rheological properties of reacting gels.

III. RHEOLOGICAL MEASUREMENTS

A. Dynamic Oscillatory Measurements

Dynamic oscillatory shear experiments, which measure the linear viscoelastic response of materials, are acknowledged to be the most valuable probes of gel or network structure. Though steady shear measurements are necessary to duplicate process conditions, the oscillatory measurements give more insight into the properties of the gel than do steady shear measurements. When interpreted using classical network theory, linear viscoelastic measurements can be used to determine the kinetics of gel formation, the crosslink density of a gel, or the shear degradation of gel structure. The gelation of polyvinyl alcohol and gelatin gels has been studied by a number of researchers (1,2,3), and at Princeton we have used these measurements to study polyacrylamide gels used as permeability control agents in enhanced oil recovery (4,5). For an introduction to the field of linear viscoelasticity the reader is referred to the text by Ferry (6).

In a linear visco-elastic measurement an oscillatory shear strain, $\gamma(t)$, is imposed on a sample,

$$\gamma(t) = \gamma_0 \sin \omega t \quad . \tag{1}$$

where γ_0 is the maximum value of the strain.

Experimentally this is accomplished by placing a sample in a cone and plate geometry, a parallel plate geometry, or between concentric cylinders in a Couette geometry, and then imposing a torsional oscillation on one plate, cone, or cylinder. The resulting stress on the stationary plate, cone, or cylinder will oscillate with the imposed frequency ω, but will be out of phase with the forcing oscillation. The measured stress can be factored into two components, one in phase with the displacement and one 90 degrees out of phase with the displacement:

$$\tau(t) = \gamma_0(G' \sin \omega t + G'' \cos \omega t) \ . \qquad (2)$$

The in-phase stress defines a storage modulus G' that gives information about the elasticity and network structure, whereas the out-of-phase component defines a loss modulus G" that gives information about the viscous or dissipative properties of the fluid. The frequency and strain dependence of the storage and loss moduli, G' and G" respectively, provide information about the state of the fluid. For an uncrosslinked guar solution both G' and G" decrease with decreasing frequency, with G" lying above G'. As a gel crosslinks G' rises until it is horizontal--independent of frequency. As an example, this progression is shown in Fig. 1 for the gelation of a polystyrene/carbon disulfide solution as temperature is decreased. As we will show in Section VI, G' can be monitored as the amplitude of the strain deformation is increased. If strain destroys the network structure, then G' will decrease with increasing strain.

Classical network theory (7) shows that G', in the low frequency region where G' is independent of frequency, is proportional to the number density of crosslinks in the gel:

$$G' = gnkT + Ge \qquad (3)$$

where g is a constant of order one, n is the number density of crosslinks, k is the Boltzmann constant, T is the absolute temperature, and Ge is a contribution to the modulus from molecular entanglements. For aqueous gels Ge is very small. It is possible to follow the kinetics of gel formation by taking the time derivative of Eq. 3:

$$\frac{dn}{dt} = \frac{1}{kT}\frac{dG'}{dt} \qquad (4)$$

Likewise, the destruction of gel structure by shear can be monitored by measuring G' after exposure to steady shear. The results can be interpreted in terms of the breakdown in the number of crosslink points.

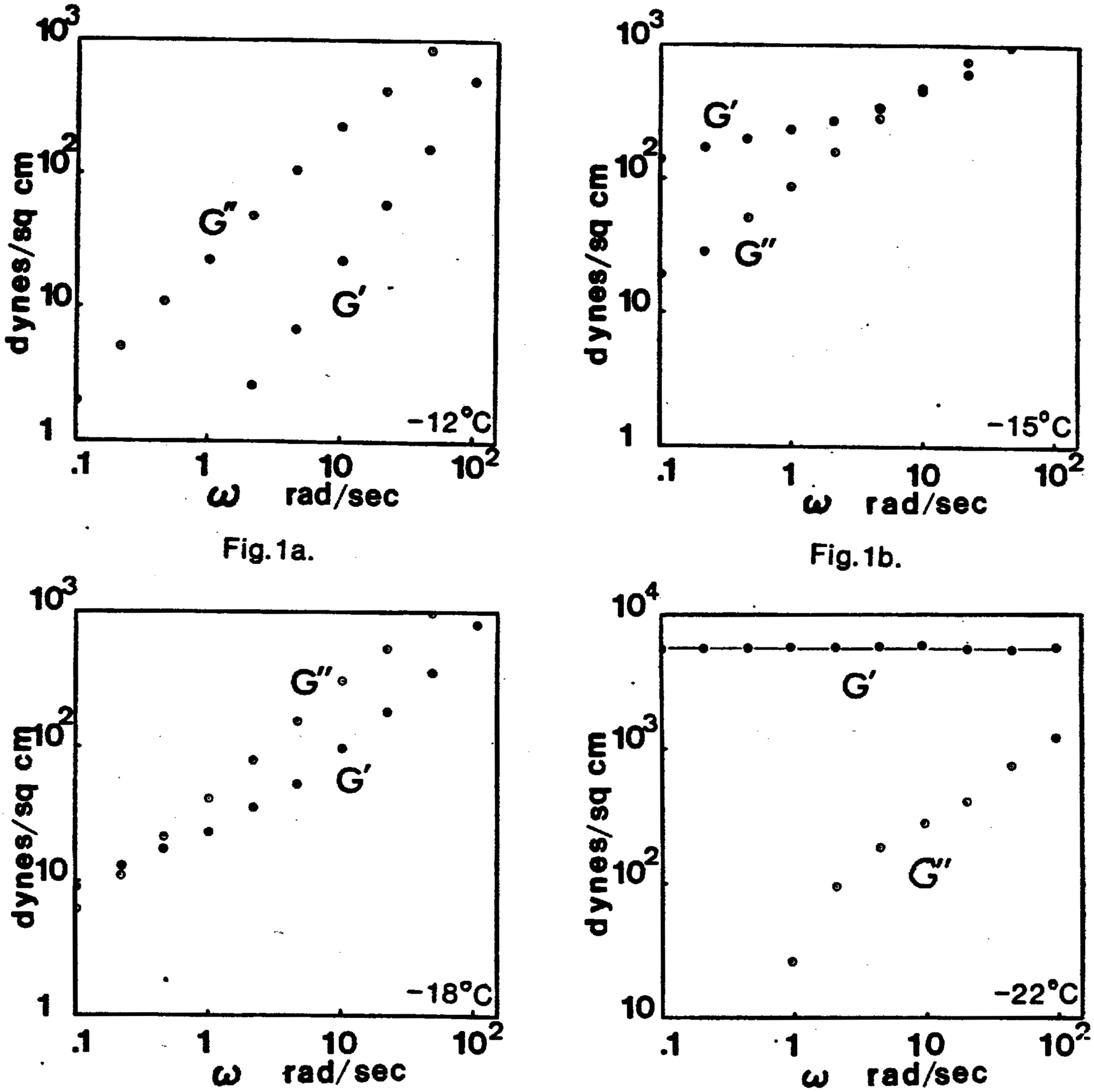

Fig.1a.

Fig.1b.

Fig.1c.

Fig.1d.

Fig.1a–d. Storage (G′) and loss (G″) moduli as a function of frequency of a 9.5 wt. % polystyrene (900,000 molecular weight) in carbon disulfide solution at temperature as indicated in each figure and run between parallel plates at 3% strain.(Clark, et.al., Polym Preprintrs 24,87(1983)).

IV. EQUIPMENT

A. Rheometrics System IV Rheometer:

Most of the measurements reported here were conducted on our Rheometrics Inc. System IV rheometer (Rheometrics, Inc., Piscataway, NJ). This state-of-the-art instrument shown in Fig. 2 has several motor and transducer options. The instrument is fully automated and all data acquisition and manipulation is under computer control. For measurements with the Fluids Transducer a circulating water bath is available with a temperature range from -20°C to 80°C.

For most of the guar solution measurements a Fluids Transducer with a 10 g-cm maximum torque and 100 g maximum normal force was used. This Fluids Transducer allows steady shear measuremements of fluid viscosity, dynamic oscillatory shear measurements, and, with a some modification to the drive unit, steady shear followed by oscillatory shear. For polymer solutions and gels the range of frequencies and shear rates over which measurements can be made is usually determined by the minimum torque range of the transducer (about 1/1000 to 1/500 of the maximum torque). Frequencies from 0.01 to 100 rad/s are accessible and steady shear rates from 0.01 to 10,000 s^{-1}. The Fluids Transducers can be run with cone-and-plate, parallel plate, or Couette geometries.

For dynamic oscillatory measurements on guar gels the 10 g-cm transducer is ideal; however, the torque range of this transducer is quickly exceeded if steady shear measurements are attempted on gels. Therefore, for the bulk of the gel measurements a Fluids Transducer with a 100 g-cm torque range was used.

For our System IV rheometer we have a high temperature and pressure cell that allows measurement of fluid viscosity and dynamic moduli under pressures to 450 psi and temperatures to 300°C. However we generally found it more convenient to perform high temperature measurements on a Rheometrics Pressure Rheometer, described below, rather then on our System IV.

B. Rheometrics Inc. Pressure Rheometer:

Measurements of gel properties at elevated temperatures were performed on a Rheometrics Pressure Rheometer located at Rheometrics Inc. laboratories in Piscataway, NJ. The instrument has a unique sealed sample chamber with a Couette geometry. Steady shear and dynamic oscillatory shear measurements over the same range of shear rates and frequencies spanned by the System IV Fluids Transducer are possible. The torque sensitivity of the Pressure Rheometer corresponds approximately to that of the 100 g-cm Fluids Transducer. It is possible to seal and pressurize the sample cell to run samples at temperatures above the normal boiling point of water. It is somewhat awkward to load and mount the sample cup -- the process takes 2-3 minutes. Modifications to allow on-line introduction of the sample to the cup have been suggested to the manufacturer.

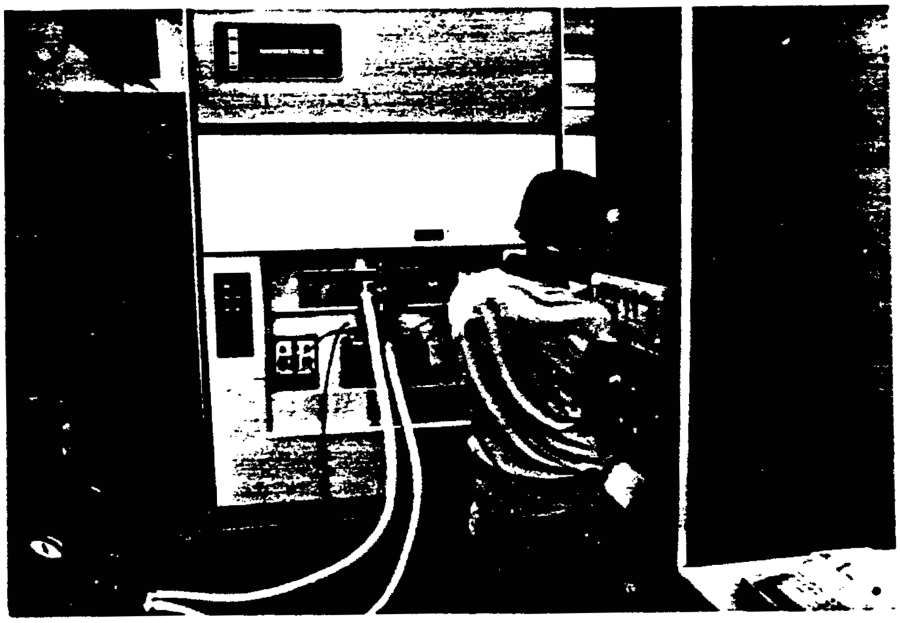

Fig.2. System IV Rheometer.

C. Impingement Mixing Device:

The homogeneity achieved during the mixing of the guar and titanate solutions and shear history of the fluid as it crosslinks determines the gel properties. The recommended procedure of mixing the guar solution and titanate solution in a blender and then transferring the preformed gel to the viscometer yields irreproducible results. This will be discussed below. To circumvent this problem, an impingement mixing device was fabricated that intimately mixes the two streams and injects them directly into the rheometer test cell (Fig. 3). The device consists of a stainless steel double acting pneumatic cylinder that is mechanically coupled to a microliter glass syringe. The pneumatic cylinder is pressurized with nitrogen at 200 psi to force guar solution in the cylinder and titanate solution in the syringe through an impingement mixing head; the mixture then flows through a packed bed mixing section. The packed bed consists of three inches of a 1/4" OD stainless steel tube packed with 24-32 mesh (0.71 - 0.50 mm) sand. During injection through the sand pack the Reynolds number is about one, based on a mean hydraulic radius for the sand pack and the viscosity of the uncrosslinked guar. The connections in the device are made with 1/8" teflon tubing. A three-way valve is used to divert fluid either to waste or to the rheometer cell. The fluid flows directly into the rheometer cell and the dynamic oscillatory measurement can be initiated even before the fluid fills the gap. The total time between the initial contacting of the guar and metal ion solutions and the start of a dynamic oscillatory experiment is on the order of 5 to 10 seconds. For a steady shear experiment the tube connecting the impingement mixer and the rheometer cup must be disconnected so that time to initiate an experiment is less than 1 minute. The schematic and parts list for the impingement mixer is given in Appendix B.

D. Capillary Viscometer:

A preliminary capillary viscometer has been designed and assembled. The shear history dependence of these gels, as shown in Section VI, convinced us that rather than making a circulating loop using a pump, a better design for our very small scale lab work would be a long capillary in which the fluid is pumped back and forth. In this way the fluid is under constant shear (excluding the short times needed to reverse the direction of the flow). The viscometer is being controlled by an IBM personal computer with a Tecmar Inc. A/D and D/A board. Further details and results on this device will be presented in future progress reports under next year's research project. The schematic of the capillary viscometer is given in Appendix C.

V. MATERIALS AND PREPARATION

The exact formulation of the guar gel was specified by the API Committee monitoring this project. Special lots of hydroxypropyl guar and Tyzor AA titanate were reserved for this study by Celanese and DuPont, respectively. The following formulation was used to produce a 40 lb/Mgal gel:

500 ml	distilled water
2.4 g	hydroxypropyl guar (Celanese SCN 9574)

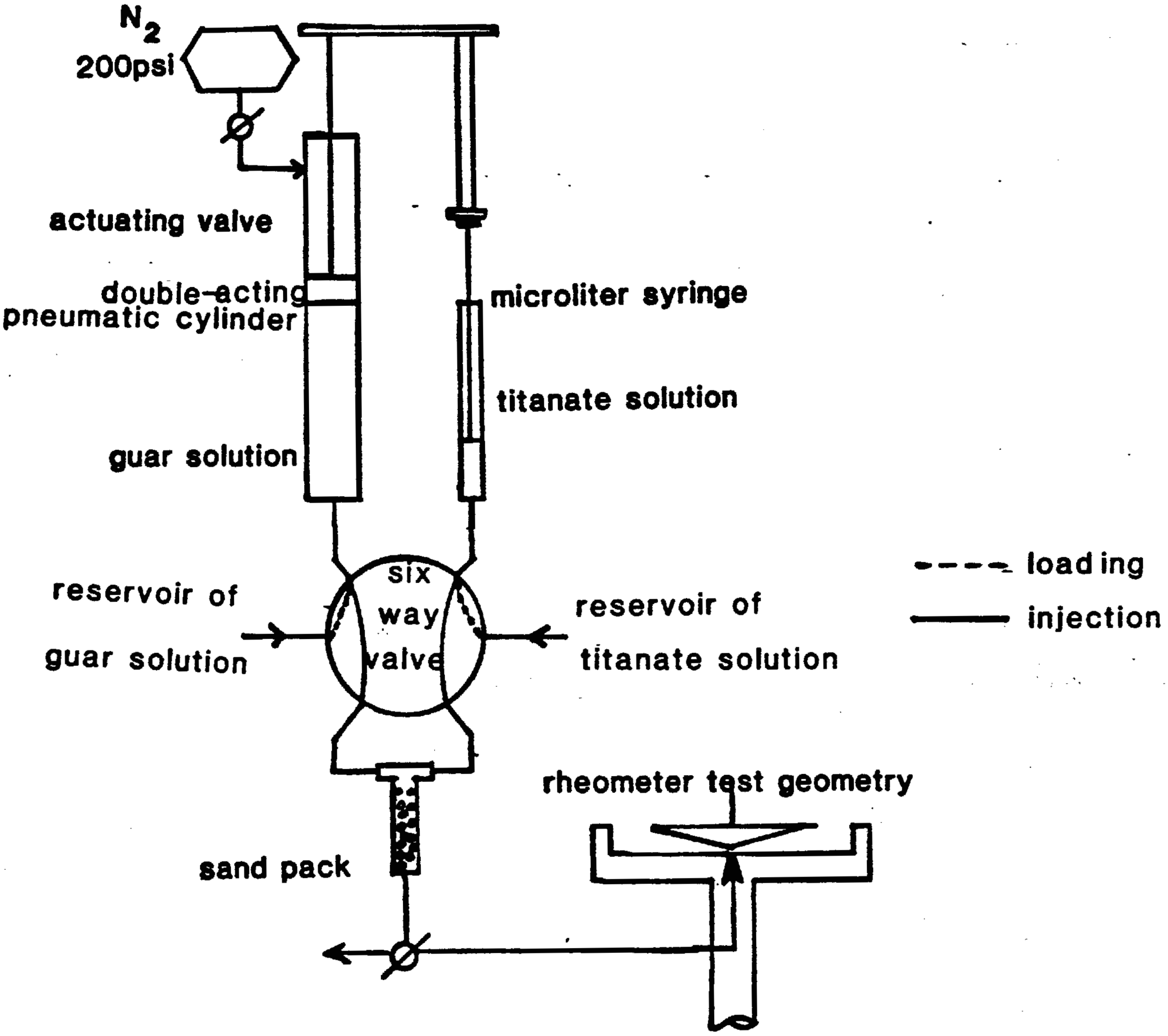

Fig.3. Impingement mixing device

0.6 g	sodium diacetate buffer (Celanese SCN 9744)
10 g	analytical grade KCL (Fisher lot 722797)
0.125 ml	25% glutaraldehyde in water (Eastman Kodak lot E11A)
2 ml	of (9:1) solution by volume isopropyl alcohol (JT Baker) and Tyzor AA titanate (DuPont)

The base guar (without crosslinking agent) is prepared using an Osterizer blender set at low speed. A timer and variac are connected with the blender in series to control mixing time and speed. The solution is prepared in the following way. The blender, with 500 ml of water in the pitcher, is set at a low speed to produce a shallow vortex. The hydroxypropyl guar is sprinkled slowly on the free surface to produce a uniform dispersion. The potassium chloride, sodium diacetate and glutaraldehyde are quickly added. The total mixing time is three minutes. The solution is then transferred to another container and allowed to mix for about 20 hours on a low shear tumbling mixer.

To prepare crosslinked guars for rheological studies two procedures were used. During the first half year the solutions were mixed by hand, and in the last half year the impingement mixing device was used. In mixing by hand, 10 ml of base guar solution is placed in a beaker, followed by a proportional amount of Tyzor AA (diluted with isopropanol). The solution is stirred vigorously with a glass stirring rod for 30 seconds and transferred into the rheometer cup. The rheometer stage is then closed to set the proper gap and the test begins. This technique proved more reproducible than mixing the guar and titanate in a blender. The good reproducibility of dynamic oscillatory measurements for samples mixed by hand is shown in Fig. 4. However, variation in the hand mixing resulted in inadequate homogenization and time delays which caused variations in steady shear measurements. This led to our development of the impingement mixer. Subsequent studies with the impingement mixer have shown that mixing also influences dynamic oscillatory measurements (Section VI.B.1a). Because it was not possible to get the cross-sections of the guar cylinder and titanate syringe in exactly the correct ratios, extra isopropanol was added to the titanate solutions to obtain the correct titanate volume for the syringe. The added isopropanol did not affect the gelation kinetics (Section V.A.5). In all cases the Tyzor AA concentration in the final gel corresonded to that specified in the recipe above.

For experiments lasting more than about 10 minutes, the free liquid surface is covered with mineral oil to prevent evaporation. The mineral oil is immiscible in the guar solution and does not affect the torque signals. Between runs the rheometer tools are cleaned with water, followed by alcohol. Thorough cleaning is required to remove oil films or the gel will prematurely slip at the tool surfaces during measurement.

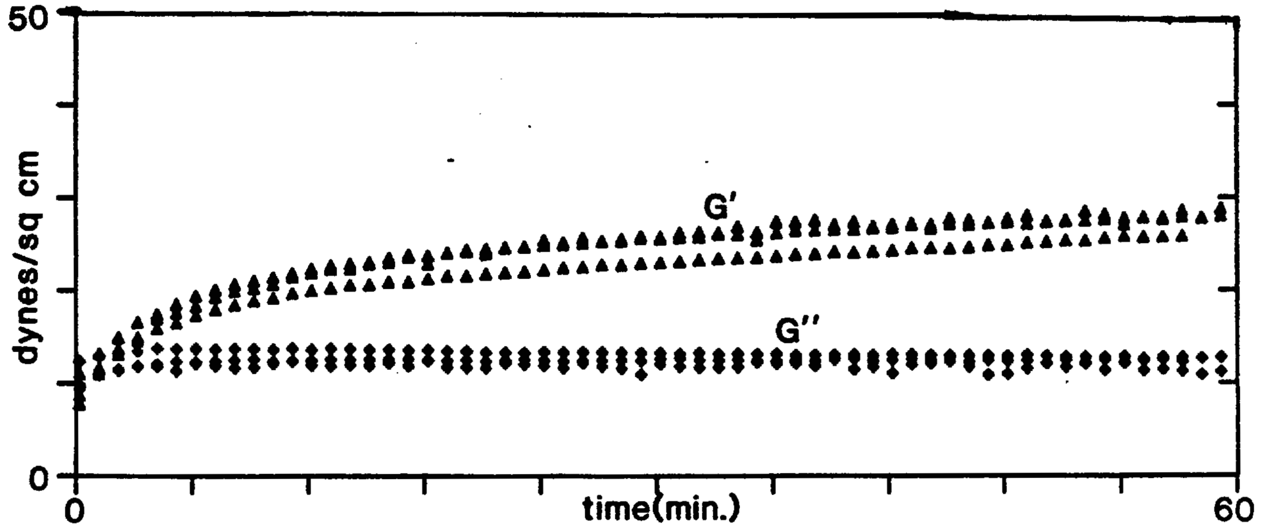

Fig.4. Test of reproducibility of gel mixing and formation at diffent times by different operators. Samples were .48% HP guar (G+K+N) mixed with Tyzor AA (.04%) by hand. Tests began immediately after mixing at 1rad/sec & 100% strain (runs 51983 3, 61083 4 & 61583 1).

VI. RESULTS AND DISCUSSION

The properties of guar gels depend on the chemistry chosen, the mixing of the components, and shear history of the gel. In this section we present the results of studies on these effects.

A summary of all of the measurements performed this year and reported to the API Committee at quarterly review meetings has been prepared by Dr. John Cameron, the Committee Vice-Chairman (Appendix D). The significant conclusions are presented here.

A. Chemical Effects

1. Hydration of HP-Guar

HP-guar molecules are not present as isolated entities but are rather contained inside an intact cell about ten microns in diameter (8). The guar derivatization is done in such a way that the cell wall is not disrupted. When the HP-guar is added to water, water penetrates the cell wall and begins to hydrate the guar. During hydration microcrystalline cellulose domains are dissolved, the cell swells, and finally the cell wall ruptures releasing the guar. The rate at which this occurs depends on pH, temperature, and the osmotic pressure difference across the cell wall. An experiment was conducted to test how long it took to fully hydrate the guar. A guar solution was prepared and mixed in the blender for 30 minutes under strong agitation. Immediately thereafter dynamic oscillatory measurements were run as a function of strain amplitude. The results in Fig. 5 show that G' decreases as strain amplitude increases. This indicates that there are three-dimensional structures in solution, probably arising from association of the unhydrated guar domains, that are easily broken down by shear. This is not observed if the guar is allowed to age 20 hours after the initial mixing. This same phenomenon is shown in Fig. 6 where, for the solution mixed 30 minutes, the steady shear viscosity increases at low shear rates, whereas for the aged solution the viscosity reaches a Newtonian plateau. This increase in low shear viscosity also indicates aggregation and structure in solution. It is important to note that at higher shear rates the viscosities of the two fluids are identical since moderate shear fields can disrupt these weak aggregates. We see that dynamic oscillatory or low shear rate measurements are sensitive probes of structure in solution.

2. Order of Addition

We were surprised to find that the order of addition of ingredients to the original base guar solution had an effect on the gels that were ultimately formed. Dr. William Stivers of Celanese (8) has suggested that this might be related to the hydration of the guar, the osmotic pressure in the solution during hydration, and the number of cells that fail to rupture. The order of addition of the sodium diacetate buffer (N), potassium chloride (K), and guar (G) was varied in a series of tests. Though no differences in the rheology of the guar solutions prepared using different orders of addition could be measured, certain orders of addition led to gels with lower levels of network structure (i.e., lower G'). The results are shown in Fig. 7 for different orders of addition. The differences in G' are quite noticeable, though G" data

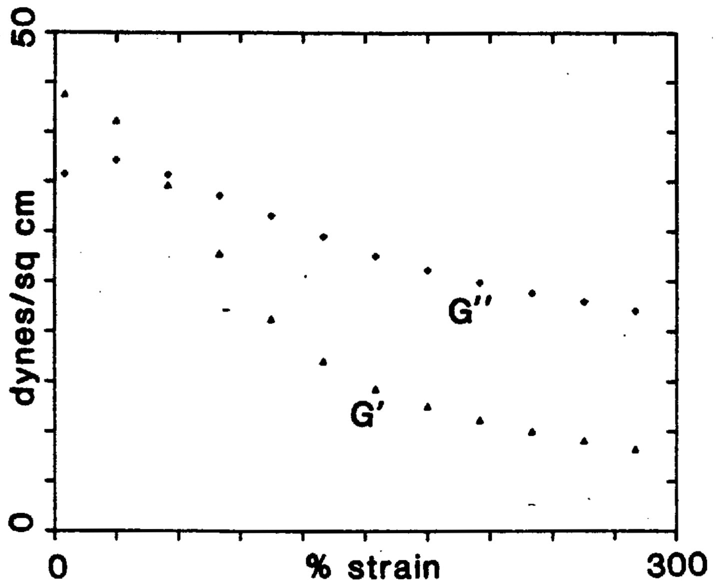

Fig. 5. Storage(G') and loss (G'') moduli as a function of strain of a .48% HP guar solution (30 minutes agitation) at 10 rad/sec (run 21783 2).

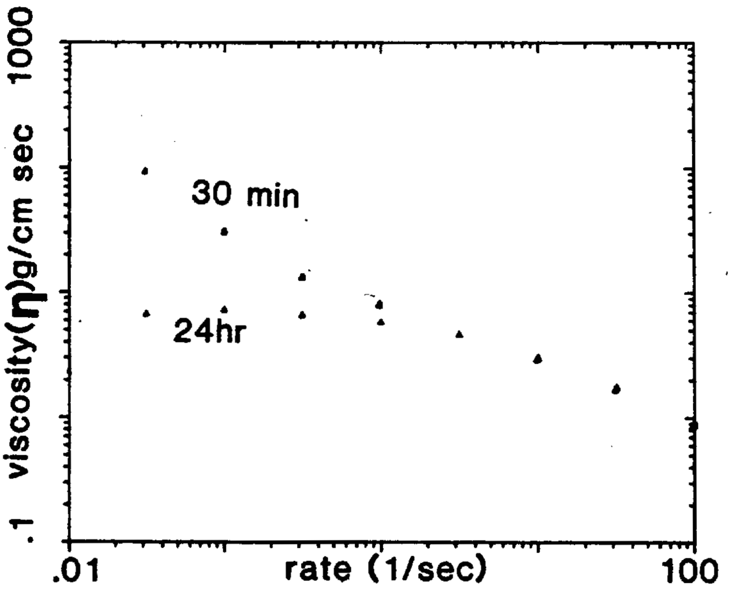

Fig. 6. Viscosity (η) as a function of shear rate of .48% HP guar solutions at different ages (runs 21683 and 21883 2).

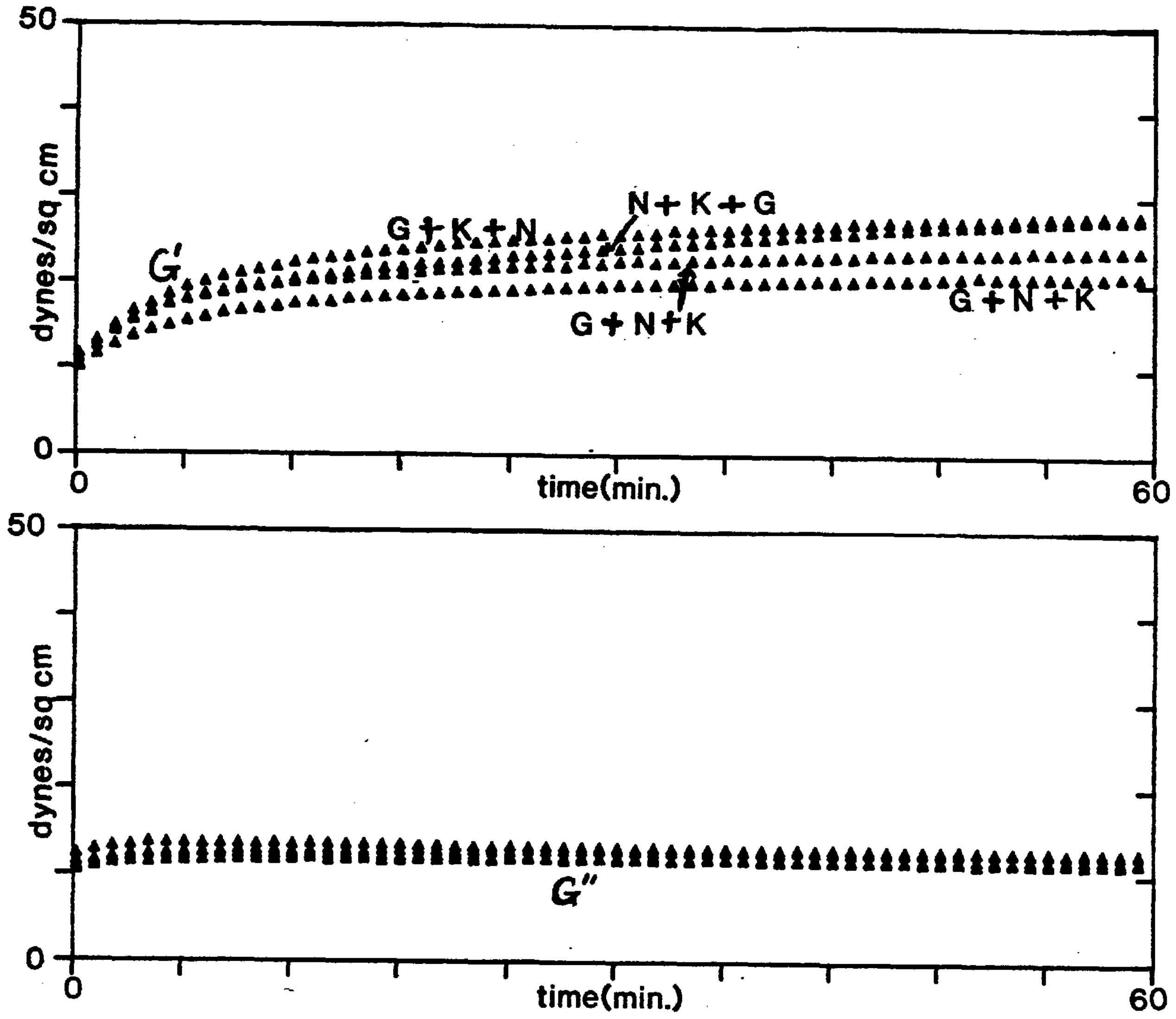

Fig.7. Effect of order of addition on G′ am and G″. of .48% HP guar mixed with Tyzor AA by hand. Measurements began immediately after mixing at 1 rad/sec and 100% strain (runs 61583 1, 61583 2, 61583 5 & 7683 2).

are similar for all runs. We have not at the time of this report duplicated these runs with the impingement mixing technique. For all subsequent studies we used the mixing order [G+K+N]. Further work on this phenomenon is underway.

3. Aging of Tyzor AA Solutions

Tyzor AA solutions change color from light yellow to orange or brown over a period of time. Dr. Donald Putzig of DuPont has suggested three mechanisms of Tyzor aging (9):

a. Photo-reduction of Titanium. This will give a green/blue color. Keeping solutions in brown bottles eliminates this problem.

b. Oxidation of Acetylacetone by Oxygen. This will give an orange color. However, Dr. Putzig did not think this would affect the crosslinking reaction.

c. Hydration of Titanium by Water from the Air. This will give a white titanium dioxide precipitate.

Dr. James Steinmetz of Kay-Fries, Inc. has suggested that color change is related to acetic acid impurities present in the acetylacetone chelate (10).

We found that gels made from Tyzor AA solutions that had been opened many times over a several month period made gels with lower values of G'. Figure 8 shows the storage modulus of gels made from newly opened bottles of Tyzor AA and from bottles that had been used for several months. To eliminate these problems the large pint bottles of Tyzor AA were divided into several smaller vials and sealed. Brown vials were used and molecular seives (W.R. Grace 3A) were added to the vial to scavenge water. This worked well and gave reproducible results that did not show the effects of aging over a period of months.

4. Diketone Addition

The most straightforward way of measuring gelation kinetics is to measure the maximum slope in the plot of G' versus time and to apply Eq. 4, as we have done previously in our study of polyacrylamide/Cr(III) gelation (5). However, as can be seen from Figs. 4, 7-9, and 13-14, the reaction rate of these guar/titanate gels is so fast that the maximum rate cannot be determined with confidence -- it occurs at too short a time.

It has been suggested that diketones can be used to slow the rate of crosslinking (11). Our results, taken at room temperature, show that not only does the addition of acetylacetone (a diketone) slow the reaction rate, but it also prevents the gel from crosslinking fully. With the addition of diketone, as shown in Fig. 9, the final value of the storage modulus is decreased. It has been suggested that increasing the temperature of these solutions might activate crosslinking. Further studies of delayed crosslinking are being pursued.

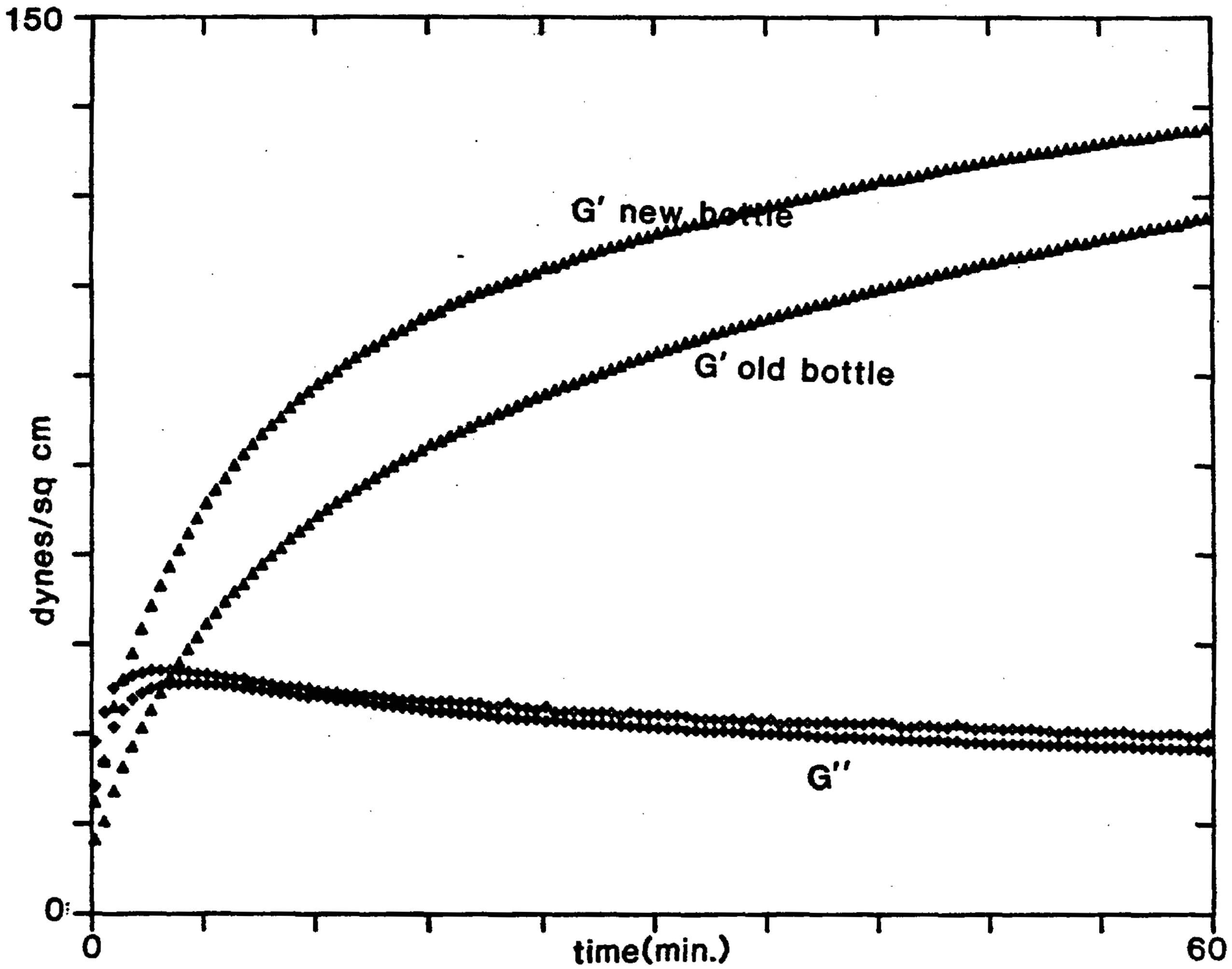

Fig.8. Storage (G') and loss (G'') moduli of HP guar gel (.48% guar (G + K + N) and .04% Tyzor AA) made from a newly opened bottle of Tyzor AA and from a bottle that had been used for several months. Impingement device was used and tests began immediately after mixing at 10 rad/sec 100% strain (runs 121583 1 & 122983 3).

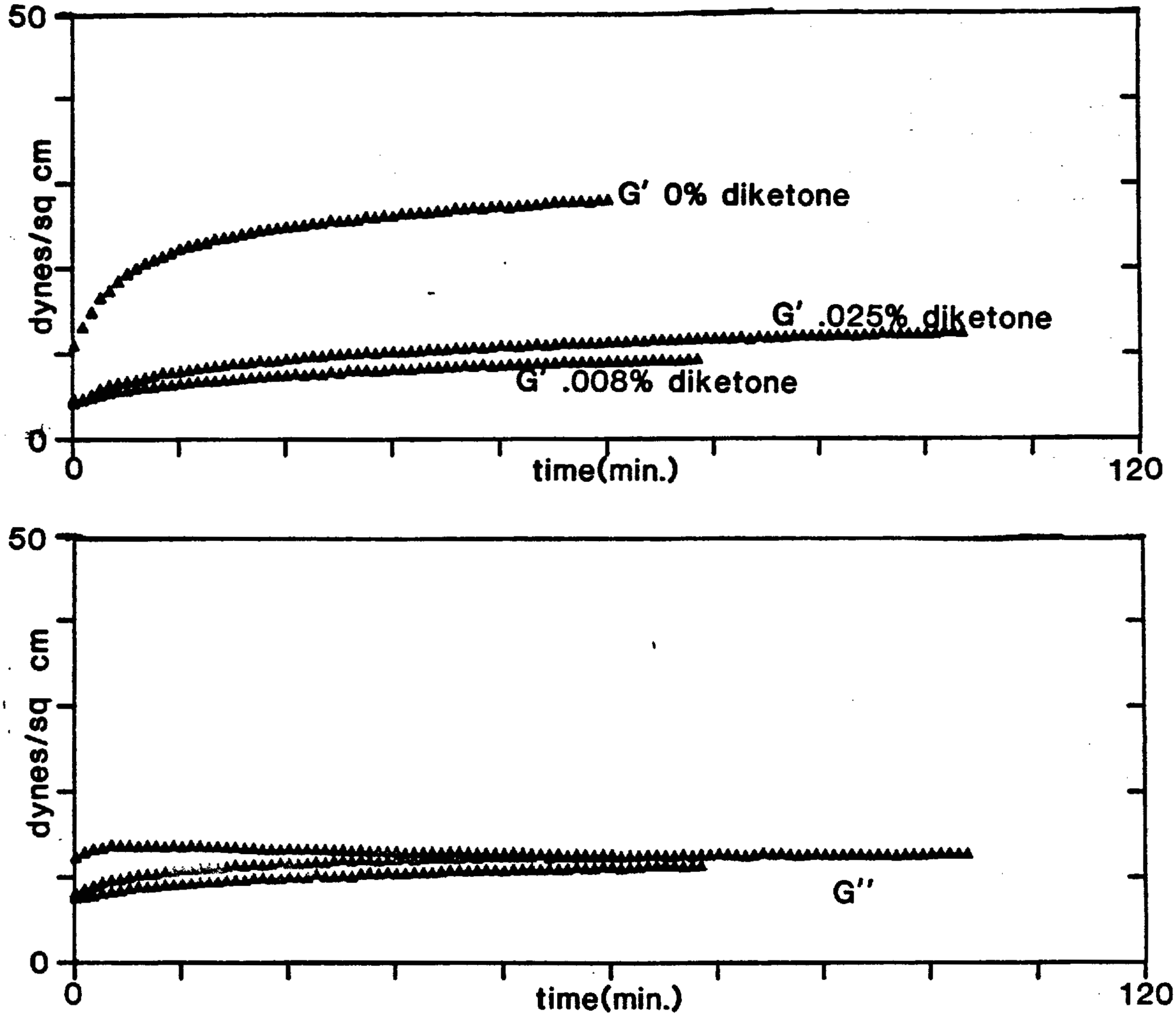

Fig.9. Effect of diketone on G' and G'' of HP guar gel (.48% guar (G + K + N) and .04% Tyzor AA). Tests began immediately after mixing by hand at 1 rad/sec and 100% strain (runs 52483 2, 52483 4 & 61583 I).

5. Isopropanol Addition

Since isopropanol is the base liquid for the titanate solution, tests were conducted on the effect of added isopropanol on gelation. Figure 10 shows G' and G" data for gels made from guar solutions with various amounts of isopropanol added before the standard Tyzor AA/isopropanol solution was added. These gels were mixed by hand. No effects of added isopropanol were detected. This showed that the Tyzor AA/isopropanol ratio in the crosslinking solution could be varied within reasonable limits as long as the same total amount of titanate was delivered. This makes matching the cross sections of the guar syringe and the titanate syringe in the impingement mixer less critical.

6. Temperature

The data reported here were taken at room temperature (23±2°C). Tests were run on the Rheometrics Pressure rheometer at 110°and 120°C, but errors from wall slip cause us to question the validity of the initial data. In the next year extensive experiments at elevated temperatures are planned.

B. Rheology of Guar Gels

In this section we present the main results on the rheology of guar gels in dynamic oscillatory and steady shear flows. The dynamic oscillatory measurements are used to characterize the network structure, whereas the steady shear measurements are intended to measure gel viscosity under process conditions.

1. Dynamic Oscillatory Measurements

a. Mixing

The degree of homogenization at a microscopic level is crucial in determining the final gel structure. The problem of mixing reactive titanium and guar solutions is in many ways analogous to problems encountered in reaction injection molding of polyurethanes in the plastics industry (12, 13). Thorough mixing in the impingement mixing device resulted in gels with lower values of G' than gels made with hand mixing. For example, the torque signal in a dynamic oscillatory test for a gel mixed by hand would be 1.1 g-cm, whereas for a gel made in the impingement mixer the torque would be 0.6 g-cm. Guar polymer chain scission during flow through the mixing device is insignificant. We believe the higher levels of elasticity noted for the hand mixed samples are caused by the inhomogeneous gel structure that is produced by incomplete mixing. During hand mixing interfaces are developed between striations or layers of bulk guar solution and the very concentrated titantate solution. The reaction rate in these interfacial regions is very high with the result that regions of dense crosslink structure are developed. The final gel formed contains microscopic threads or sheets of more highly crossliked guar that are elastic, imparting to the gel a higher level of G' than would be predicted if the crosslinks were homogeneously distributed. Characterization of the state of mixedness during the production of gels in the laboratory or field is critical.

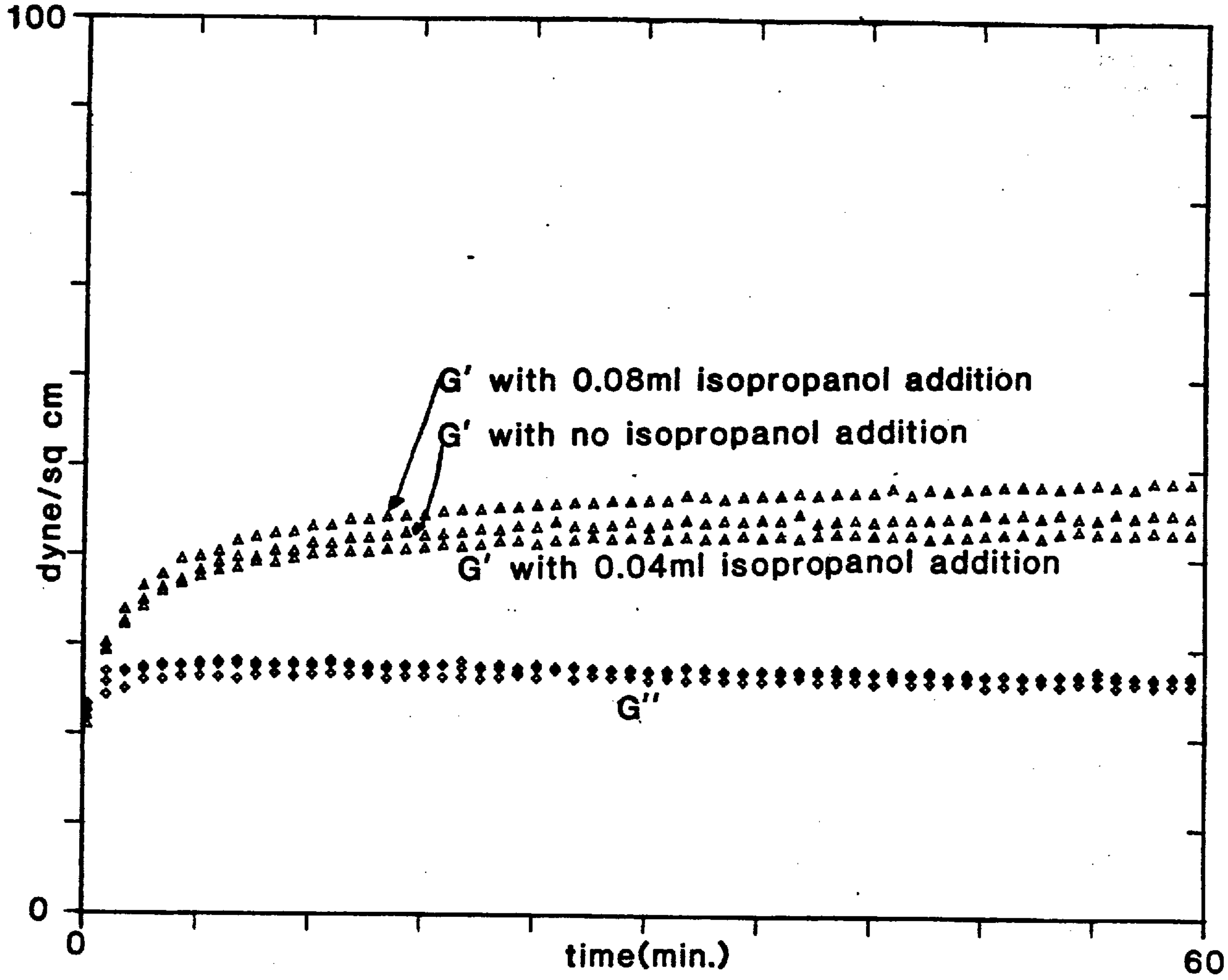

Fig.10. Effect of isopropanol addition on G' and G'' of HP guar gel (10ml of .48% guar (G+K+N) and .04ml of 10% Tyzor AA) produced by hand mixing (runs 71684 1, 71684 2, & 71684 3).

b. Storage Modulus Versus Strain Amplitude

Figure 11 shows the effect of strain on guar gels produced in the impingement mixer, introduced into the gap between parallel plates, and allowed to sit for 15 minutes before the dynamic oscillatory test at 10 rad/s was begun. At low strains the value of G' is above G". As the strain amplitude is increased G' drops dramatically indicating that the guar gel structure is being disrupted by strain or that wall slip is occurring. In this experiment the strain is first increased to 500 % and then decreased. Hysteresis can be observed indicating that in the time scale of these experiments the gel does not reheal. The necessity of having adequate torque signals requires that most of our experiments were run at 100 % strain. It should be kept in mind that at these strains some disruption of gel network structure occurs. In the next year of this study a new sensitive transducer will be available to allow measurements at lower strains. The strain sensitivity of guar gels is in sharp contrast to the perfectly elastic behavior of polyacrylamide gels formed with chromium crosslinks (5) shown in Fig. 12. The value of G' is unaffected by strains as large as 500 % for polyacrylamide gels.

c. Storage Modulus Versus Frequency

The storage and loss moduli of guar gels produced in the impingement mixer, allowed to sit for 20 minutes, and measured at 100 % strain are as shown in Fig. 13. The storage modulus, G', is above the loss modulus, G", and G' becomes constant at low frequencies as is indicative of a crosslinked gel.

d. Storage Modulus Versus Time: Chemical Kinetics

As described in Section III, by measuring the time dependence of the storage modulus during crosslinking it is possible to follow the chemical kinetics of the gelation reaction. The equilibrium modulus, which is equal to the storage modulus G' at <u>zero frequency</u> and <u>zero strain</u>, is proportional to the number density of crosslinks. From the data showing the strain and frequency dependence of these guar gels it should be remembered that at 10 rad/s the actual value of G' at zero strain is higher than the measured value. A second effect acts in opposition to the decrease in G' with strain -- the measured G' at 10 rad/s is actually higher than the equilibrium modulus of the gel as can be seen from Fig. 13. Most measurements were taken at 10 rad/s and 100% strain because those values yielded adequate torque signals and a fast data acquisition time so that reaction dynamics could be followed.

A series of measurements of the storage modulus versus time were made while varying guar and titanate concentrations (Figs. 14 and 15). The gels were produced in the impingement mixer and introduced directly into the gap between parallel plates. The time between the mixing of the guar and titanate streams and the first datum point is approximately 10 s. Measurements were conducted at 10 rad/s and 100% strain. The surprising thing about the results is the speed of the reaction. We were unable to measure an induction period before the network formed. The maximum rate of reaction (i.e. maximum slope in G' vs t) occurs before the first data point. Using the entire shape of the G' versus time curve, and interpreting this curve using the polymer kinetic theory model developed in Section VII, it should be possible to determine reaction kinetics.

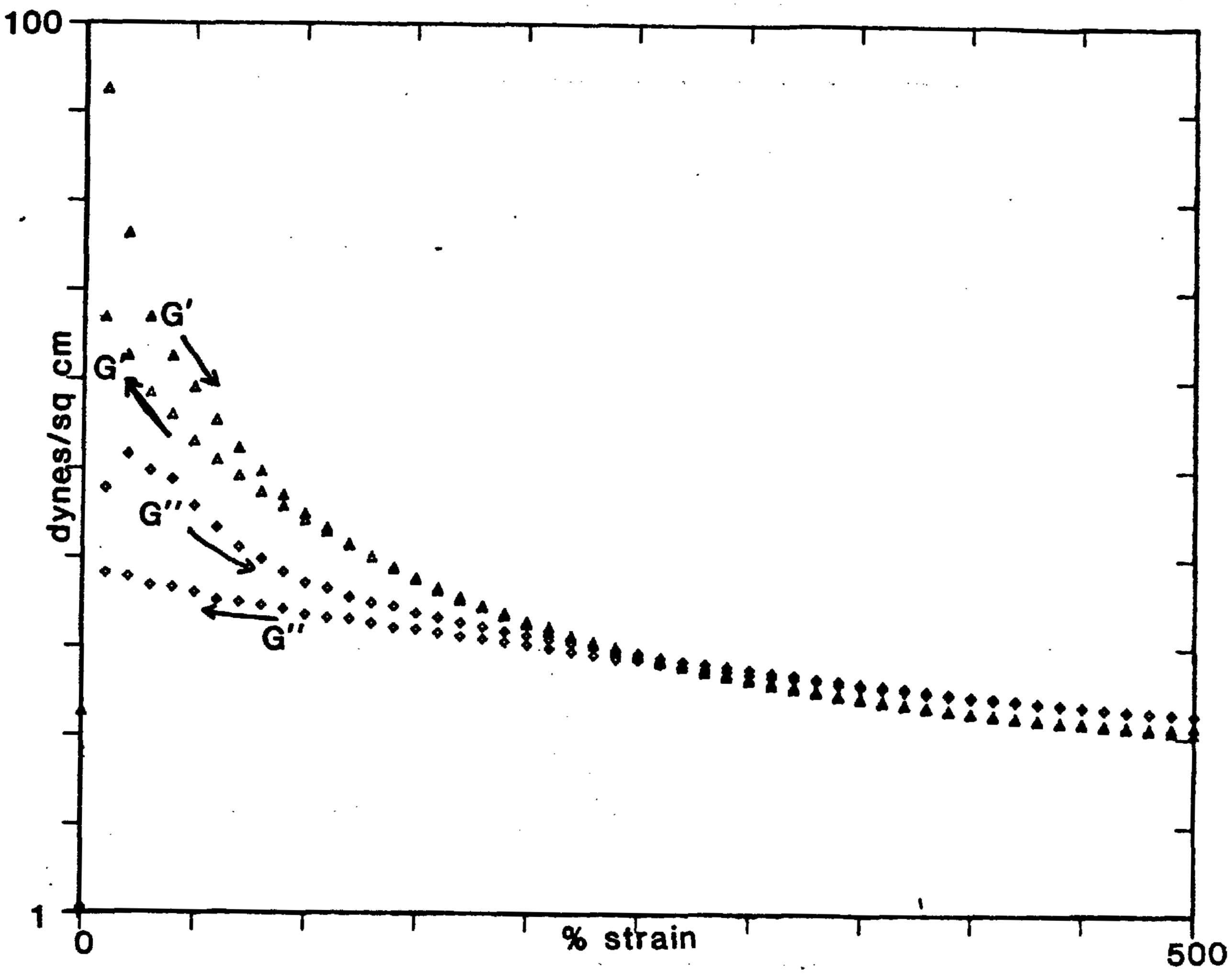

Fig. 11. Effect of strain on G' and G'' of HP guar gel (.48% guar (G+K+N) and .04% Tyzor AA) produced in the impingement device. Mixture was allowed to sit for 15 minutes before tests began at 10 rad/sec (run 113083 1). Arrow indicates the direction of strain sweep.

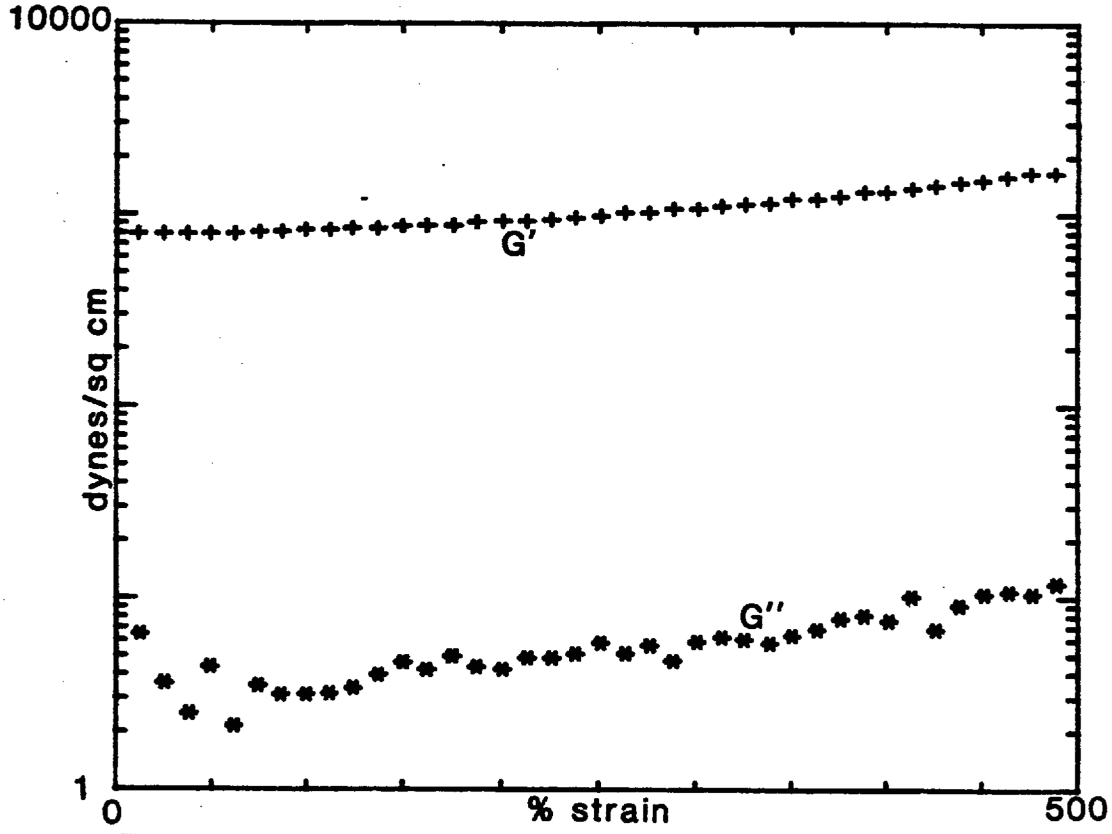

Fig.12. Effect of strain on G' and G'' of polyacrylamide gels formed with chromium crosslinks.(5).

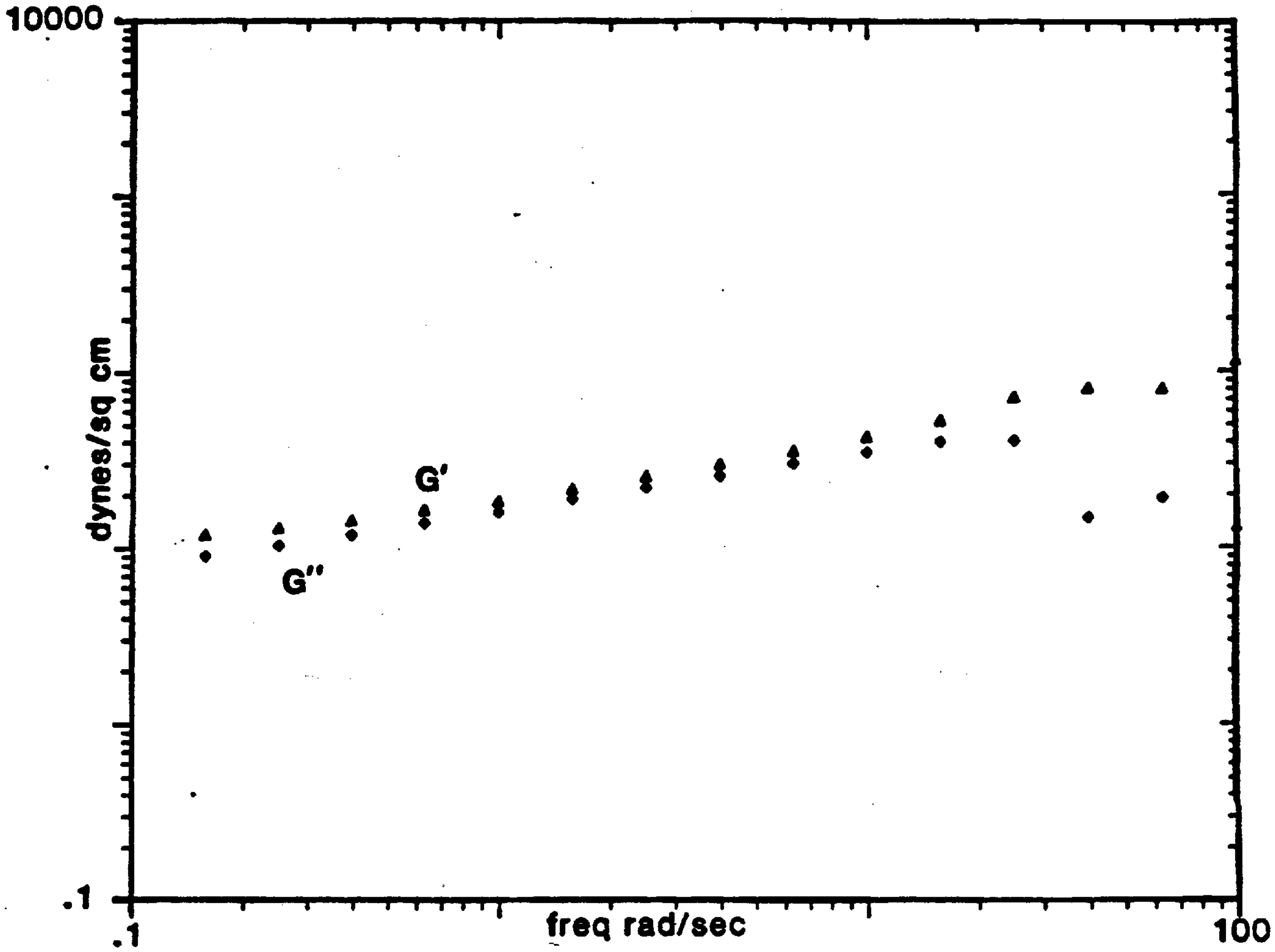

Fig. 13. Effect of frequency on dynamic moduli of .48% HP guar (G+ K+ N) gel (.04% Tyzor AA) produced in the impingement device . Mixture was allowed to sit for 20 minutes before measuring at 100% strain (run 113083 4).

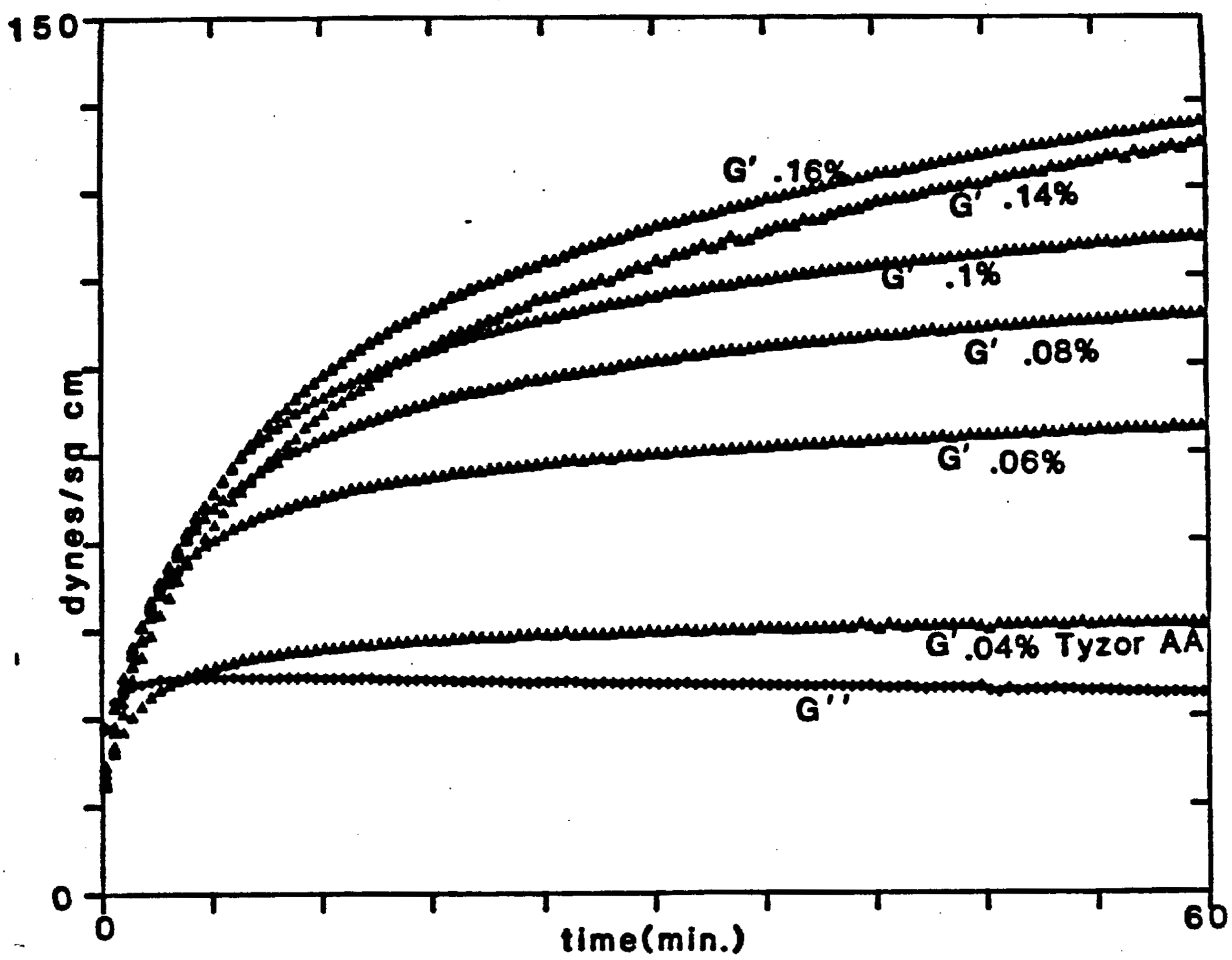

Fig. 14. Effect of Tyzor AA concentration on HP guar (G + K + N) gel formation at a constant HP guar concentration, .48%. Tests began immediately after mixing in the impingement device. Only the values of G" of HP guar (.0.48%) with .04% Tyzor AA is shown because G" are the same for all runs.(runs 122883 2, 122883 1, 122883 4, 122883 3, 122983 2,& 122983 3).

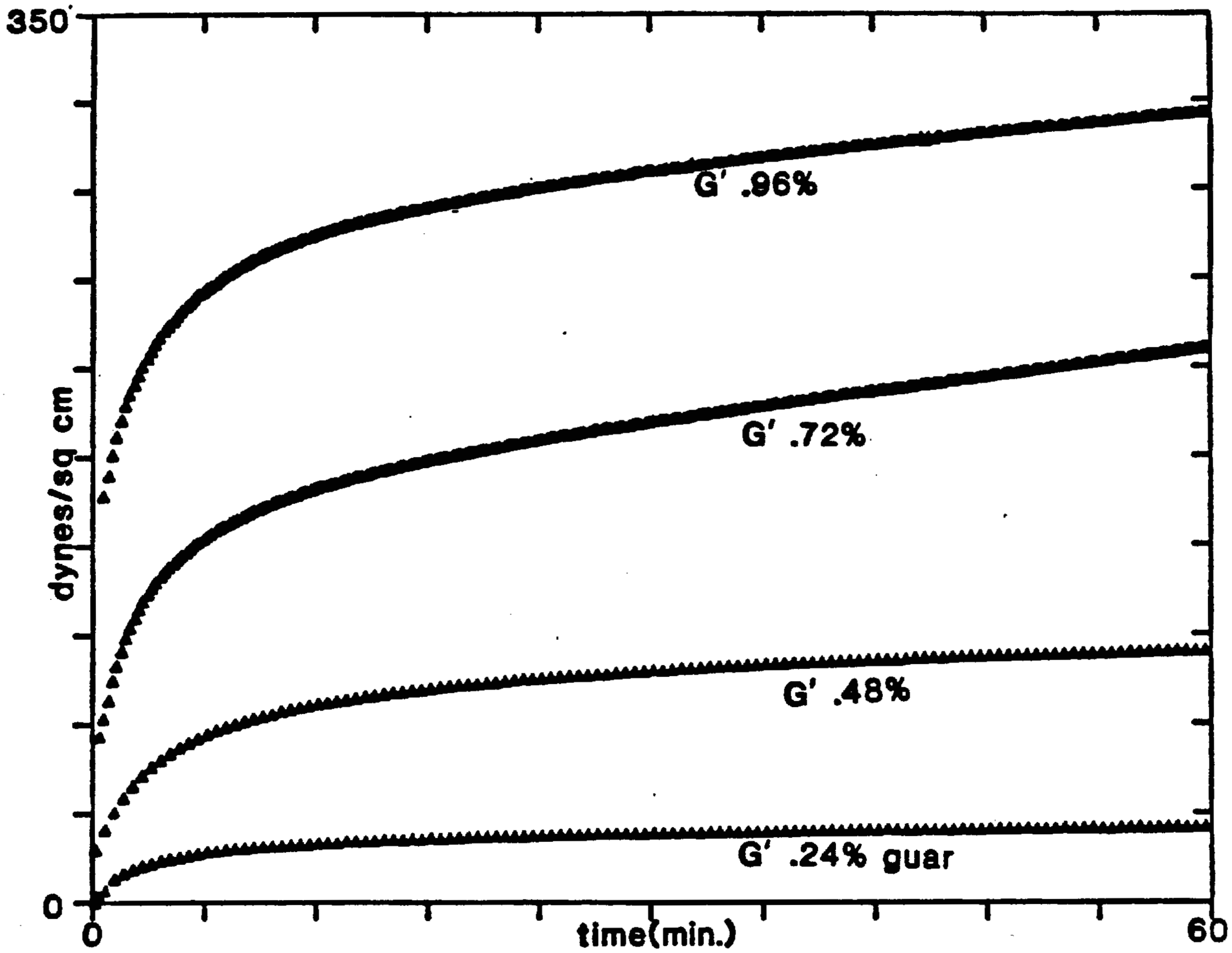

Fig.15. Effect of HP guar (G+K+N) concentration on gel formation at a constant Tyzor AA concentration, .08%. Tests began immediately after mixing in the impingement device. (runs 122883 4, 1484 3, 1484 1, & 1584 1).

These data can be used to show the sensitivity of guar gel properties to guar and titanium concentrations. It is possible to obtain the same values of G' from solutions having different compositions. However, these gels may show different time, temperature, and shear stabilities.

2. Steady Shear Measurements

a. Gels Mixed by Hand

Our initial steady shear experiments were on guar gels mixed by hand and introduced to the rheometer test cell. This process takes on the order of 2 minutes to accomplish. The quiescent period before steady shear is imposed, we now believe, has a dominant effect on the viscosity that is measured. The stress versus time behavior for gels being sheared at 100, 500, and 1000 s^{-1},respectively were investigated. Several series of tests were run where the gels were allowed to sit 2.5, 3.5, and 4.5 minutes before shear was initiated. In all of the steady shear experiments the asymptotic stress at long times (1500 s) is roughly the same - independent of shear rate. When the stress data is divided by shear rate to obtain a viscosity, η_∞, a log-log plot of viscosity versus shear rate has a slope of -0.96 shown in Fig. 16. This slope is unrealistic for a polymer fluid (which normally has a slope between -0.6 and -0.3), and is much more suggestive of wall slip. Each η_∞ datum point on Fig. 16 represents a new experiment. Stepping up or down in shear rate to obtain η_∞ at several shear rates for the same gel introduces shear history effects and will produce different results. A standard procedure to test for the presence of wall slip is to take two sets of measurements with different gap settings. If, at the same shear stresses, the shear rates are the same with both gaps, then wall slip is thought not to occur; but if, at the same shear stresses, the shear rate in the narrower gap is greater, then slip is occurring. We performed steady shear measurements at 25 s^{-1} with gaps of 0.75 mm, 1.5 mm, and 3.0 mm as shown in Fig. 17. In all cases the shear stresses at long times were identical within experimental uncertainty. This indicates slip is not occurring. The interpretation of these observations is uncertain. Resolution will require direct measurement of the velocity field. We consider this a major research need at this point.

b. Impingement Mixing: Effect of Shear on Reaction Rate

By using the impingment mixer it is possible to introduce solutions into the rheometer and begin measurements before the fluid completely gels. A series of measurements at 25, 100, and 500 s^{-1} were run and the results of stress versus time are shown in Fig. 18. In the runs at 25 and 100 s^{-1} the stress increases linearly for 100-200 s as the guar network gels. At the gel point the fluid can no longer flow and the stress rises sharply. It then falls just as sharply, as would be observed if the gel broke away from the parallel plate surfaces and began to slip. After the drop in stress it remains essentially constant for 1500 s. The location of the rise in stress and also the slope of the stress versus time plots for 25 and 100 s^{-1} increases with increasing shear rate. The conclusion is that shear increases the rate of reaction. We may assume that for the measurement at 500 s^{-1} the jump in stress at very short times corresponds to the gel point which is seen more clearly at the lower shear rates.

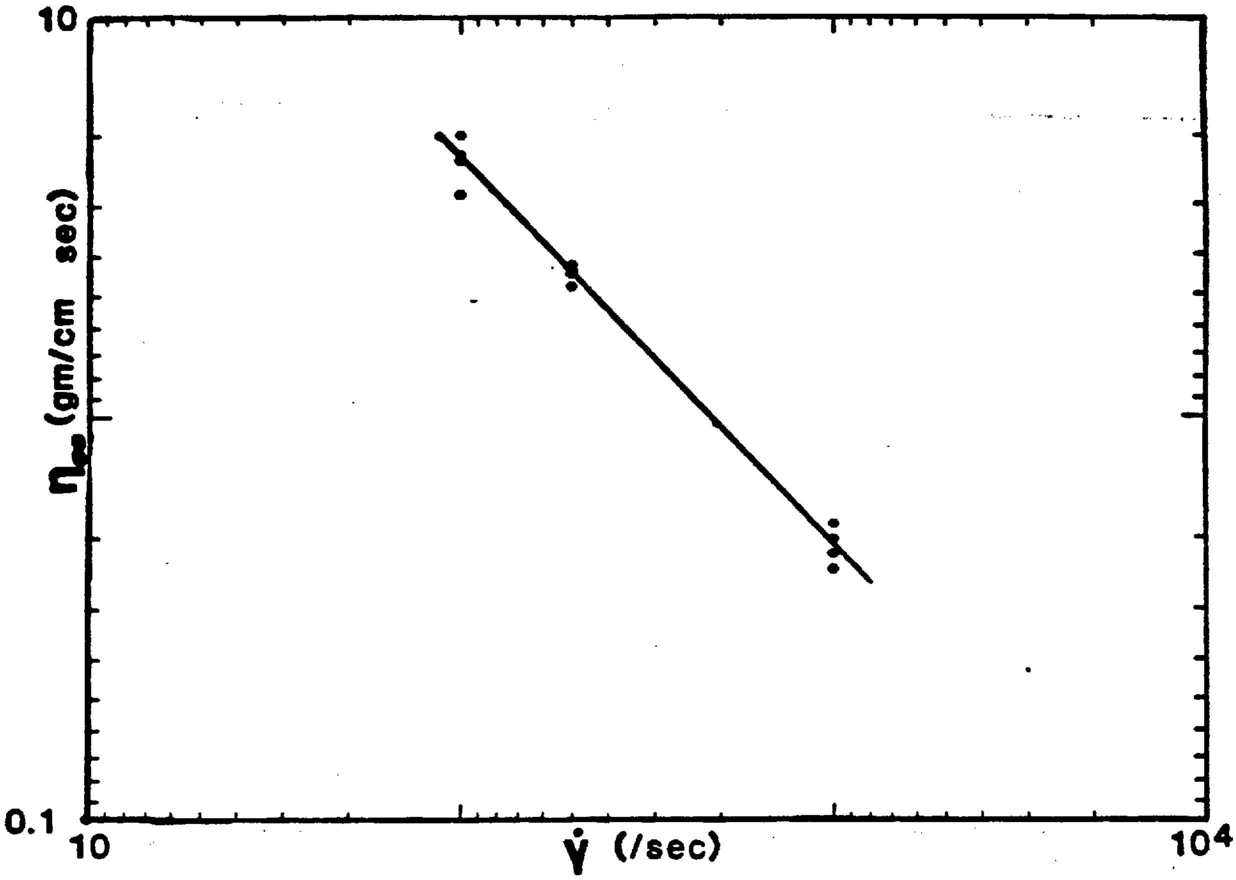

Fig.16. Effect of shear rate on viscosity (η_∞) of .48% HP guar (G + K + N) gels with .04% Tyzor AA produced by hand mixing. Tests began after the gels were allowed to sit 2.5 , 3.5 and 4.5 minutes. Solid line is a least squar fit of these points. (runs 81683 1,81683 2, 81683 3, 81683 4, 81683 5, 81683 6, 81783 1, 81783 2, 81783 3, 81983 1 81983 2, & 81983 4).

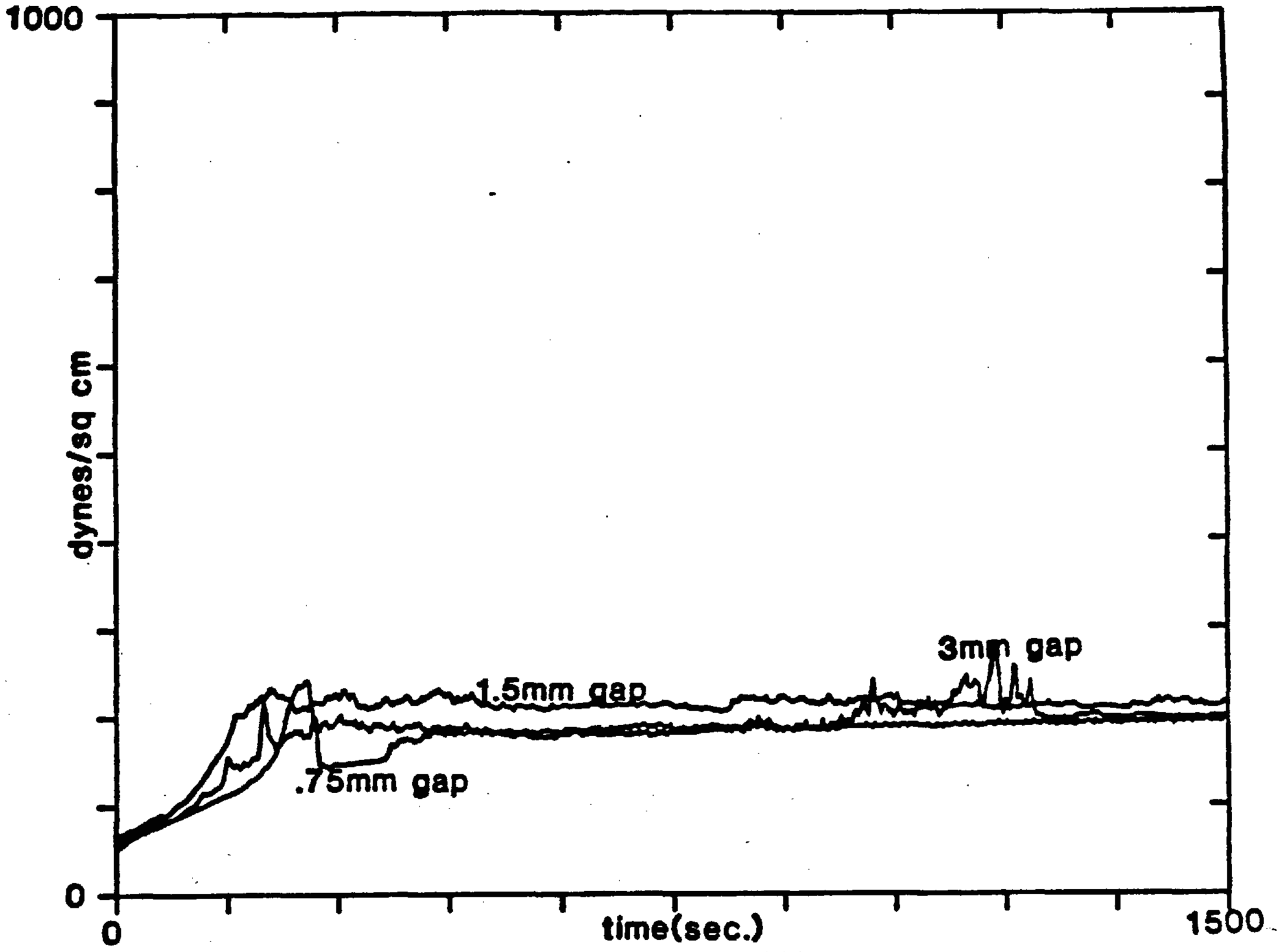

Fig.17. Steady shear measurements with parallel plates geometry with gaps of 0.75mm, 1.5mm & 3.0mm on .48% guar (G+K+N) gels (.04% Tyzor AA) produced in the impingement device. Tests began immediately aftter mixing at 25/sec.(runs 11084 1, 11184 1 &11184 2).

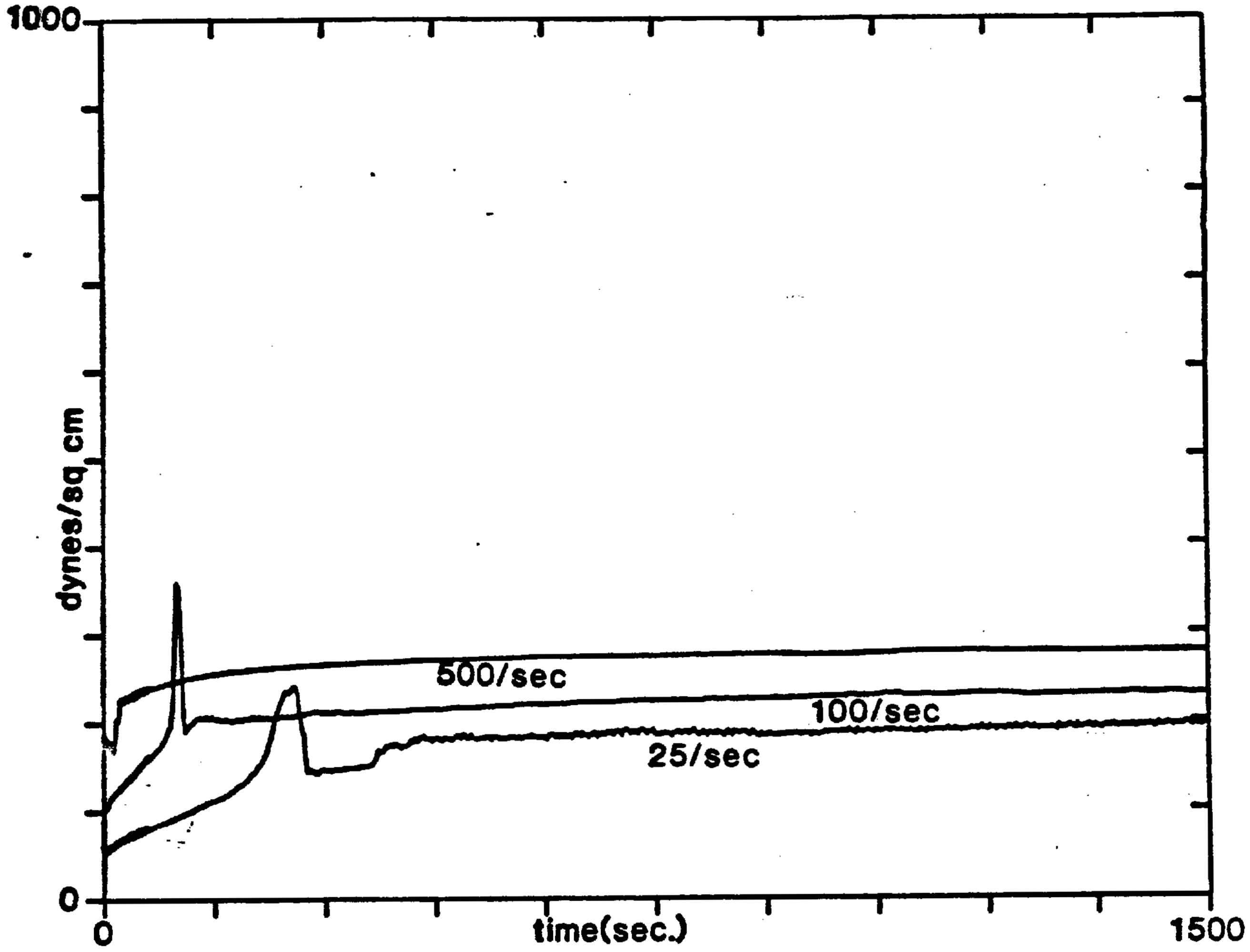

Fig.18. Effect of shear on reaction rate of gel formation. Samples were .48% guar (G+K+N) gels (.04% Tyzor AA) produced in the impingement device. Tests began immediately after mixing at various shear rates with .75mm gap.(runs 11084 3, 11184 1 & 11184 4).

This behavior has not been reported by previous investigators because the gel point is reached before the gel can be mixed and loaded into a Fann viscometer.

c. Steady Shear Followed by Oscillatory Shear

Measurements were made both with our System IV rheometer and with the Rheometrics Pressure Rheometer on the effect of steady shear followed by dynamic oscillatory shear. In these tests the samples were mixed by hand. Figures 19 and 20 show the stress versus time and modulus versus time data, respectively, for an experiment that consisted of alternating periods of 1000 s^{-1} shear for 60 seconds and dynamic oscillatory shear at 100 % strain and 10 rad/s for 60 seconds. The steady shear portion shows a gradual increase in stress level and after each period of dynamic testing the stress spikes and decays rapidly. The stress overshoot when the steady shear is reapplied may be due to either rehealing of the the gel network or rebonding of the network to the tool surfaces during oscillatory shear. This suggests that flow loop devices with regions of quiescent fluid may lead to results that are not indicative of flow under constant shear, and this was one of the reasons we chose a reciprocating capillary viscometer design.

VII. KINETIC THEORY MODELING

A. Background

The kinetic theory for the rheology of fluids with temporary network junctions has been developed by researchers attempting to model the flow of entangled polymeric fluids (14-19). In this previous work the junctions were envisioned as temporary entanglement points that would form and disengage in response to flow. We have extended the theory by incorporating the reaction of the titanium with the guar polymer and subsequent crosslinking of guar molecules. The temporary entanglements in the classical theory are replaced by the chemical crosslinks in the guar gel system. The theory allows one to calculate the constitutive equation for the reacting gel in explicit form. This equation can then be used to calculate the dynamic oscillatory response of a gel and the shear viscosity as a function of time under shear histories duplicating process conditions.

Crosslink formation appears to consist of two steps: first, the attachment of the metal ions to the polymer backbone, followed by the formation of crosslinks between adjacent chains through metal-ion bridges. This latter step is most probably reversible and depends on flow history. Thus, a network theory coupled with chemical reaction kinetics is essential to predict the rheology of guar gels. We present here a model that incorporates both of these steps -- chemical kinetics controls the formation of active sites for crosslinking, and the rate of junction formation is given by the product of the rate of polymer chain collision and the probability that a collision will lead to a crosslink. The model is based on the Bird-Carreau network model (14, 15) with the addition of chemical reaction kinetics to describe the formation of chemical crosslinks among the polymer molecules in solution. This model has the ability to predict an increase in storage modulus with time, shear thinning viscosity, stress overshoot upon the inception of shear flow, and viscosity changes during flow history simulation of fracturing operations.

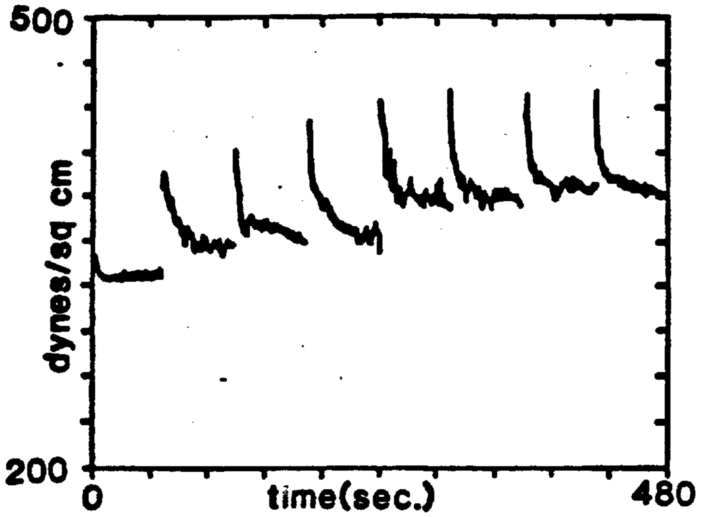

Fig.19. Stress vs. time for an experiment that consisted of alternating periods of 1000/sec shear for 60 sec. and dynamic oscillatory shear at 100% strain and 10 rad./sec. for 60 sec. Sample was .48% HP guar (G+ K+ N) gel with .04% Tyzor AA mixed by hand (run 51183 5).

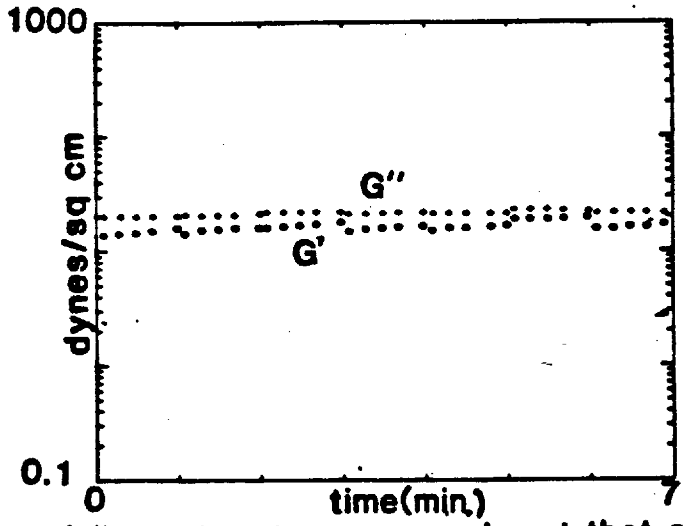

Fig.20. Dynamic moduli vs. time for an experiment that consisted of alternating periods of 1000/sec. shear for 60 sec. and dynamic oscillatory shear at 100% strain and 10 rad/sec. for 60 sec. Sample was .47% HP guar (G+ K+N) gel with .04% Tyzor AA mixed by hand.(run 51183 5).

B. Network Theories

As a common starting point in network theories for macromolecular fluids, the equation for stress in a deformed network is derived from rubber elasticity theory (7, 15). In what follows we adopt the nomenclature of Bird, Hassager, Armstrong, and Curtiss (15), henceforth denoted BHAC. The stress tensor is given by,

$$\underline{\underline{\tau}} = -gnkT\underline{\underline{\gamma}}_{[0]} \tag{5}$$

where g is a parameter of order one, n is the number density of crosslinks, k is the Boltzmann constant, T is the absolute temperature and $\gamma_{[0]}$ is the Finger tensor describing the deformation of the material (BHAC, p. C-3, C-4). To pass from the theory for an elastic solid (that is, a permanently crosslinked network) to a fluid for which the crosslink junctions form and break during flow, a model must be developed to account for the change in the number density of crosslinks with time. The theory is formulated not in terms of crosslinks, but rather chain segments between crosslinks. It is, therefore, possible to distinguish between chain segments of various lengths or kinds. A population balance on the number density of chain segments of kind j formed at time t' that still exist at a later time t" is given by,

$$\frac{\partial}{\partial t''} n_{t''t'j} + \hat{\lambda}_j^{-1} n_{t''t'j} = 0 \tag{6}$$

where $n_{t''t'j}dt'$ is the number of segments of kind j per unit volume in the network at time t" created in the time interval from t' to t' + dt', and $\lambda_j^{-1}dt$ is the probability that a segment of kind j created at some past time t' is lost in the time interval from t" to t" + dt".

The junction balance equation, Eq. 6, is solved subject to the initial condition that at time t" = t' there is a net rate of creation of segments,

$$n_{t't'j} = \hat{\eta}_j \hat{\lambda}_j^{-2} \tag{7}$$

where $\hat{\eta}_j \hat{\lambda}_j^{-2}dt'$, is the number of segments of kind j that are created per unit volume in the time interval t' to t' + dt'.

The stress in an elastic network strand depends on its extension. For the temporary junction model the extension depends both on the rate of deformation and the length of time the strand has been undergoing deformation. The original equation for the stress tensor, Eq. 5, must be integrated over all past time to account for the creation of network junctions at past time that still exist at the present time. Also, the contributions from all of the j-kinds of strands is summed to obtain:

$$\underline{\underline{\tau}}(t) = \sum_{j=1}^{\infty} \int_{-\infty}^{t} n_{t\ t'j}\, kT \underline{\underline{\gamma}}_{[0]}\, dt' \qquad (8)$$

Thus for the classical network theories of polymer fluids Eq. 6 is solved to obtain the junction kinetics, and Eq. 8 is solved to obtain the stress tensor. The main modeling problem comes in the selection of the parameters η and λ, which represent the rate of junction destruction and the rate of junction creation, respectively.

At this point different authors propose different empirical expressions for the kinetic parameters η and λ. If they are assumed constant, then the Lodge "rubber-like'liquid" is obtained (18). Unfortunately, this model is incapable of describing shear thinning viscosity or stress overshoot, as well as other important phenomena. To correct this deficiency Kaye (17) assumed the parameters are functions of stress. Kay's model leads to an integro-differential equation for stress for which no closed-form solution is available and for which even numerical evaluation is difficult. Bird and Carreau (14-16) proposed letting η and λ depend on the second invariant of the rate of strain; that is $\sqrt{(\gamma:\gamma)/2}$. Physically this implies that junction creation and destruction is a function of the rate of energy dissipation in the system. This results in a closed form expression for stress in terms of the velocity gradient in shear flow. The model has been extensively tested and fits both linear viscoelastic and non-linear material properties well. The model and its development are outlined below because the extension of the model to include chemical kinetics follows directly from the Bird-Carreau model.

In the Bird-Carreau model the rates of loss and creation of segments in the network are assumed to be functions of shear rate. Thus, Eq. 6, a balance on the segments in the network at time t" in the interval t'<t"<t, give,

$$\frac{\partial}{\partial t} n_{t"t'j} + \hat{\lambda}_j(\dot{\gamma}")^{-1}\, n_{t"t'j} = 0 \qquad (9)$$

where $\dot{\gamma}" = \dot{\gamma}(t")$.

Carreau introduced empirical expression for the η_j and λ_j:

$$\hat{\eta}_j(\dot{\gamma}) = \eta_j h_j(\dot{\gamma}) \qquad (10)$$

$$\hat{\lambda}_j(\dot{\gamma}) = \lambda_j g_j(\dot{\gamma}) \qquad (11)$$

$$\eta_j = \eta_0 \frac{\lambda_j}{\Sigma\lambda_j} \qquad (12)$$

$$\lambda_j = \frac{2^{\alpha}\lambda}{(j+1)^{\alpha}} \tag{13}$$

$$h_j(\gamma) = \frac{1}{1+(2^{\alpha}t_1\dot{\gamma})^{2s}/(j+1)^{2\alpha}} \tag{14}$$

$$g_j(\gamma) = \frac{[1+(\lambda\dot{\gamma})^2]^R}{1+(2^{\alpha}t_1\dot{\gamma})^{2s}/(j+1)^{2\alpha}} \tag{15}$$

Notice that there are six constants in this model: η_0, λ, α, t_1, s, and R. The first three parameters can be determined from linear viscoelastic measurements; the other three may be determined from measurements of the nonlinear behavior of the material.

Carreau's expression for junction kinetics can be coupled with the equation of state for stress, Eq. 8, to solve for the material functions:

viscosity :

$$\eta = \sum_{j=1}^{\infty} \eta_j h_j \tag{16}$$

primary normal stress coefficient:

$$\theta = 2\sum_{j=1}^{\infty} \eta_j h_j \lambda_j g_j \tag{17}$$

dynamic moduli :

$$G'' = \sum_{j=1}^{\infty} \frac{\eta_j \omega}{1+(\lambda_j\omega)^2} \tag{18}$$

$$G' = \sum_{j=1}^{\infty} \frac{\eta_j \lambda_j \omega^2}{1+(\lambda_j\omega)^2} \tag{19}$$

C. Constitutive Equation for Reactive Network Fluids

In this modified Bird-Carreau model incorporating chemical reaction kinetics, the stress is still assumed to be determined by the number density of crosslinks. The stress tensor is then given by Eq. 8. The same differential equation governing the balance of segments, Eq. 6, is also used. In the population balance equation the nature of the chemical crosslinks determines the value of the kinetic parameter λ_j, which is associated with the rate of crosslink destruction. No additional term is added to the segment balance equation to account for chemical reaction, because segments once created at past time t' can be destroyed only at some later time t"; that is, at some present time t" segments cannot be created that have a past history of (t" - t'). The chemical reaction kinetics come into the solution of the differential equation through the initial condition that at t" = t', which specifies the net rate of creation of segments.

The adsorption of metal ions onto the polymer backbone is assumed to be the precursor of chain-chain crosslinks formation. Thus, the initial condition for the solution of Eq. 8 includes the chemical kinetics of this process. The initial condition is given by,

$$\text{at time } t'' = t' : \eta_{t't'j} = \hat{\eta}_j(\dot{\gamma}')\hat{\lambda}_j^{-2}(\dot{\gamma}')P \qquad (20)$$

Collisions between polymer chains occur at a rate $\eta_j\lambda_j^{-2}$ as in the Carreau model; however, there is probability P that the collision produces an effective crosslink. The probability can be thought of as the "stickiness" of the polymer chain which will depend on the fraction of adsorption sites on the polymer backbone that have reacted with metal ions.

Let us assume that the probability of a chain-chain collision creating a junction is directly proportional to the fraction of sites on the polymer chain that are occupied by metal ions. The fraction of filled sites is S. If the reaction for this adsorption process is first order, then:

$$\frac{dS}{dt} = K(1 - S) \qquad (21)$$

where 1/K is the time constant for the adsorption reaction. With the initial condition that at time equal to zero no sites are filled, Eq. 21 can be solved for S:

$$S = 1 - \exp(-Kt) \qquad (22)$$

Therefore, the probability of a chain-chain collision creating a junction is [1 - exp(-Kt)]. The reaction rate constant K can be obtained from the time dependence of the storage modulus of a crosslinked gel as will be shown below. The initial condition for the network junction equation is then:

$$\text{at } t'' = t' : \eta_{t't'j} = \hat{\eta}_j(\dot{\gamma}')\hat{\lambda}_j^{-2}(\dot{\gamma}')[1 - \exp(-Kt)] \qquad (23)$$

The material functions for a reacting network fluid are obtained from the solution of Eqs. 6 and 8, subject to the initial condition in Eq. 23.

D. Material Function in Shear Flow

1. Dynamic Oscillatory Shear

Consider a material subject to the oscillatory velocity field given by,

$$v_x = \dot{\gamma}_0 \, y \cos\omega t \tag{24}$$

where the velocity is in the x-direction and the gradient of the velocity is in the y-direction:

$$\dot{\gamma}_{yx} = \frac{dv_x}{dy} = \dot{\gamma}_0 \cos\omega t \tag{25}$$

The xy-component of the Finger tensor for oscillatory shear is given by (Ref. 10, p. C-3):

$$\left(\underline{\underline{\gamma}}_{[0]}\right)_{xy} = \frac{\dot{\gamma}_0}{\omega} \left(\sin\omega t' - \sin\omega t\right) \tag{26}$$

In the linear viscoelastic regime the junction kinetics and material functions are independent of the magnitude of the rate of strain, $\dot{\gamma}_0$, and depend only on frequency ω. Therefore, following Bird and Carreau we factor $\lambda_p(\dot{\gamma})$ and $\eta_p(\dot{\gamma})$ each into two terms, a constant prefactor and strain rate independent term which goes to unity in the linear viscoelastic limit:

$$\begin{aligned} g_p(\dot{\gamma}) &\rightarrow 1 \qquad \text{as } \dot{\gamma} \rightarrow 0 \\ h_p(\dot{\gamma}) &\rightarrow 1 \qquad \text{as } \dot{\gamma} \rightarrow 0 \end{aligned} \tag{27}$$

The shear stress can be obtained analytically from the solution of Eq. 9 for the junction kinetics with Eq. 23 as the initial condition and Eqs. 10-15 for the kinetic parameters. For small amplitude oscillatory motion the shear stress, τ_{xy}, is given by:

$$\begin{aligned} \tau_{xy} = \frac{\dot{\gamma}_0}{\omega} \sum_j \frac{\eta_j}{(\lambda_j)^2} \Big\{ \Big[& \frac{-\lambda_j^3 \omega^2}{1 + \lambda_j^2 \omega^2} + \frac{\lambda_j^2}{\lambda_j - \tau} \exp\left(-\frac{t}{\lambda_j}\right) \\ & - \frac{\tau\lambda_j}{\lambda_j - \tau} \exp\left(-\frac{t}{\tau}\right) + \frac{\tau\lambda_j(\lambda_j - \tau)\exp(-t/\tau)}{(\lambda_j - \tau)^2 + (\tau\lambda_j\omega)^2} \Big] \sin\omega t \\ & + \Big[-\frac{\lambda_j^2 \omega}{1 + \lambda_j^2 \omega^2} + \frac{\tau^2 \lambda_j^2 \omega \exp(-t/\tau)}{(\lambda_j - \tau)^2 + (\tau\lambda_j\omega)^2} \Big] \cos\omega t \end{aligned}$$

$$\underline{+ \left[\frac{\omega\lambda_j^2}{1+\lambda_j^2\omega^2} - \frac{\lambda_j^2\tau^2\omega}{(\lambda_j-\tau)^2+(\tau\lambda_j\omega)^2} \right] \exp\left(-\frac{t}{\lambda_j} \right) \} } \qquad (28)$$

where $\tau = 1/K$. No singularity occurs as $\tau \rightarrow \lambda_j$, which can be proved by using L'Hopital's rule. The underlined transient term is associated with the start-up of flow at $t = 0$, and it disappears quickly, because normally λ_j is in the order of seconds (Carreau 1972). The transient response associated with the chemical reaction is of a much longer time scale. Thus, the dynamic moduli are:

$$G" = \sum_j \frac{\eta_j}{\lambda_j^2} \left[\frac{\lambda_j^2\omega}{1+\lambda_j^2\omega^2} - \frac{\tau^2\lambda_j^2\omega\exp(-t/\tau)}{(\lambda_j-\tau)^2+(\tau\lambda_j\omega)^2} \right] \qquad (28)$$

$$G' = \sum_j \frac{\eta_j}{\lambda_j^2} \left[\frac{\lambda_j^3\omega^2}{1+\lambda_j^2\omega^2} - \frac{\lambda_j^2}{\lambda_j-\tau}\exp(-t/\lambda_j) + \frac{\tau\lambda_j}{\lambda_j-\tau}\exp(-t/\tau) \right.$$

$$\left. - \frac{\tau\lambda_j(\lambda_j-\tau)\exp(-t/\tau)}{(\lambda_j-\tau)^2+(\tau\lambda_j\omega)^2} \right] \qquad (29)$$

It can be seen that G' (eq. 33) rises to its final equilibrium value with a tim constant given by the rate of chemical reaction, $\tau(=1/K)$. Figure 21 shows G' versus time which mimics the experimentally obtained G' data for crosslinking guar gels.

2. Steady Shear Flow

For a material in a velocity field given by,

$$v_x = \dot{\gamma}_0 y \qquad (30)$$

the velocity gradient is:

$$\dot{\gamma}_{yx} = \dot{\gamma}_0 \qquad (31)$$

For this steady shear flow, the modified Carreau's model gives the steady viscosity, η, and the primary normal stress coefficient, θ, as:

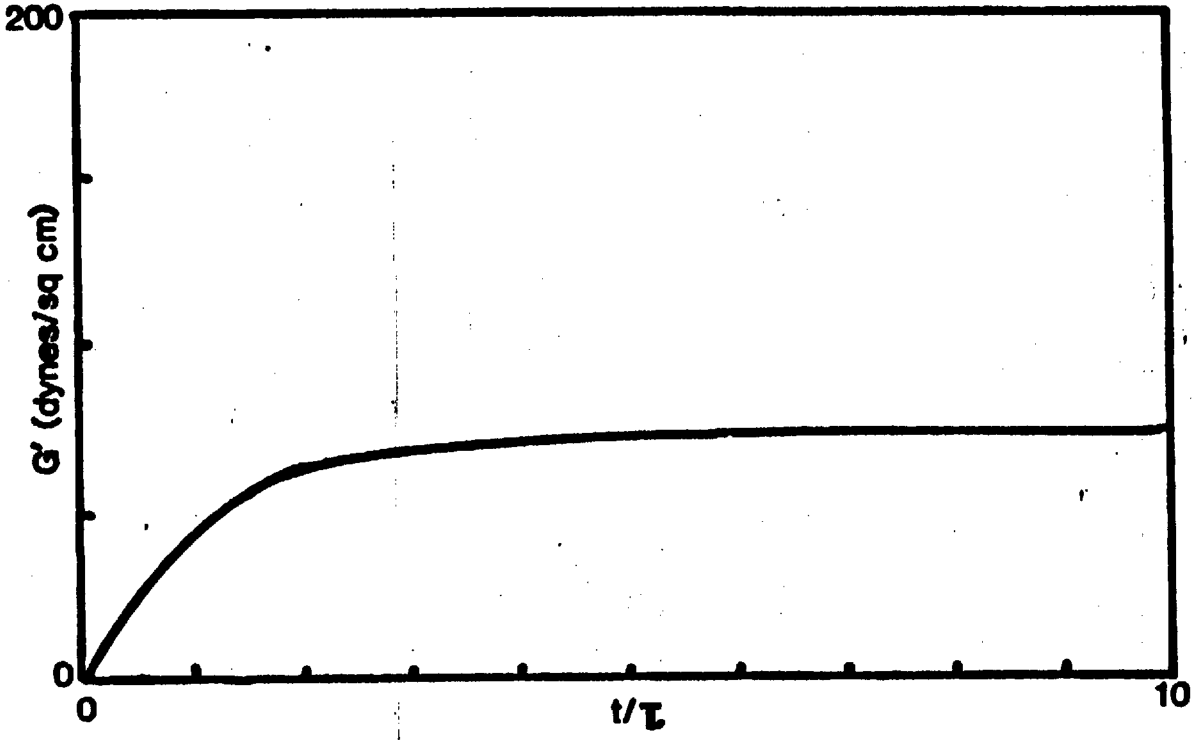

Figure 21. Pridictions of storage modulus (G') vs. t/τ with parameters: η_0 = 250 N.s/m^2, α = 2.7, λ = 4.078, S = 0.863, R = 0.1605, t_1 = 2.923 s, τ = 100 s, and w = 1 rad./s.

$$\eta = \sum_j \{\eta_j h_j - \frac{\eta_j h_j}{(\lambda_j g_j)^2} \exp(- \frac{t}{\lambda_j g_j}) [\lambda_j g_j t + \lambda_j^2 g_j^2$$

$$+ t \frac{\lambda_j g_j \tau}{\lambda_j g_j - \tau} + (\frac{\lambda_j g_j \tau}{\lambda_j g_j - \tau})^2 \exp(- \frac{\lambda_j g_j - \tau}{\lambda_j g_j \tau} t) - (\frac{\lambda_j g_j \tau}{\lambda_j g_j - \tau})^2 \} \quad (32)$$

$$\theta = \sum_j \frac{\eta_j h_j}{(\lambda_j g_j)^2} \{2\lambda_j^3 g_j^3 - \exp(- \frac{t}{\lambda_j g_p}) [\lambda_j g_j t^2 + 2\lambda_j^2 g_j^2 t + 2\lambda_j^3 g_j^3$$

$$+ \frac{\lambda_j g_j \tau}{\lambda_j g_j - \tau} t^2 - 2t(\frac{\lambda_j g_j \tau}{\lambda_j g_j - \tau})^2 + \frac{2(\lambda_j g_j \tau)^3}{(\lambda_j g_j - \tau)^3}$$

$$- \frac{2(\lambda_j g_j \tau)^3}{(\lambda_j g_j - \tau)^3} \exp \left(- \frac{\lambda_j g_j - \tau}{\lambda_j g_j \tau} t \right)] \} \quad (33)$$

The shear viscosity predicted by Eq. 32 versus shear rate at a number of times during the gelation process in Fig. 22. That no singularity occurs as $\lambda_j g_j \to \tau$ can be proved by expanding,

$$\exp \left(- \frac{\lambda_j g_j - \tau}{\lambda_j g_j \tau} t \right) .$$

At infinite time, which corresponds to the condition of the original Bird Carreau model, Eqs. 29, 30, 38, and 39 simplify to Eqs. 18, 19, 16, and 17, respectively. This is a cross-check between our results and those of Bird Carreau.

Further work is underway on the viscosity of gels under varying shear histories to model field operating conditions.

VII. RECOMMENDATIONS FOR FUTURE RESEARCH

Detailed proposals for continued research are presented in the renewal request we have submitted to the API. Major areas of investigation are:

1. Stability of Gel Structure:

The stability of gel structure and rheology under shear and at elevated temperatures will be investigated.

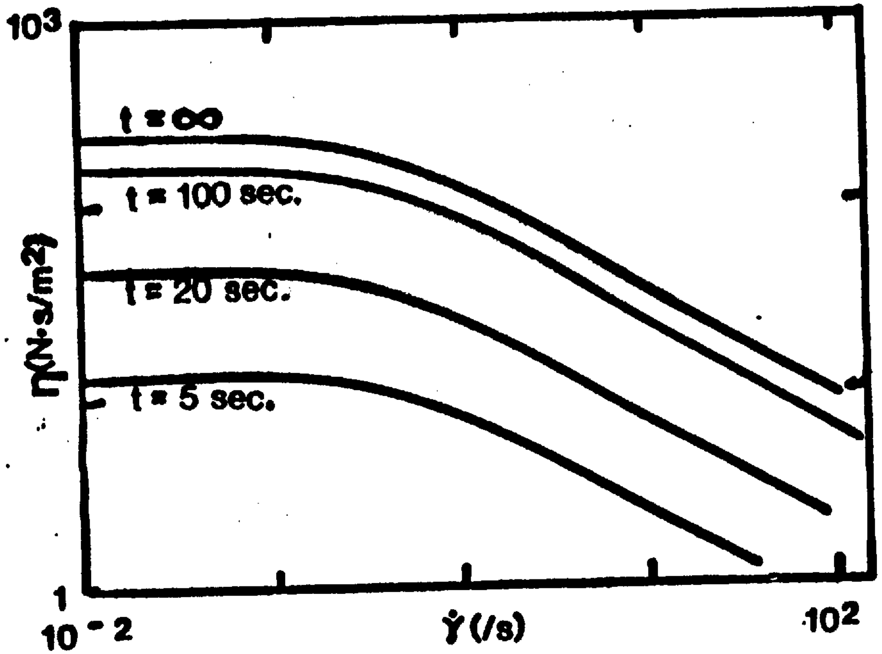

Figure 22. Predictions of steady viscosity (η) vs. shear rate ($\dot{\gamma}$) measured at different time with the parameters given in the caption to figure 21.

2. Effect of Wall Slip on Rheological Characteriztion of Gels:

Our steady shear measurements indicate that wall slip is occurring for guar gels at room temperature. The magnitude of the wall slip velocity and its dependence on gel chemistry, flow history, wall roughness, and the materials of construction of the wall must be known before the steady shear measurements can be accurately interpreted. To do this we will be conducting laser-doppler anemometer studies on gels to measure local velocity profiles.

3. Comparison of Capillary and Rotational Viscometer Viscosity Measurements:

Once the effect of wall slip has been quantified, then viscosity measurements from the capillary viscometer and the System IV rheolometer will be compared.

4. Modeling Gel Rheology:

The network model for the rheology of a reacting fluid has been presented in Section VII. Work is in progress to extract the chemical kinetics parameters from rheological data, and to test the forms of the rheological parameters taken from the Bird-Carreau model. Alternate, more complex, chemical kinetics for the titanate-guar associate may be required to get quantitative agreement with experimental data.

IX. RECOMMENDATIONS FOR INSTRUMENTATION

From our study we have seen that both dynamic oscillatory and steady shear measurements are necessary to characterize fracturing fluid gels. Rheological instrumentation that provides for both measurements includes the Contraves Low Shear 30 Sinus (Tekmar Co., Cincinnati, OH), the Haake CV 100 (Haake, Inc., Saddle Brook, NJ), the Weissenberg-Sungamo Rheogoniometer (Sungamo Transducers, Grand Island, NY), the Rheometrics System IV Rheometer (Rheometrics, Inc., Piscataway, NJ), Rheometrics Fluids Rheometer, and the Rheometrics Pressure Rheometer. The Fann 35 and Fann 50 viscometers, which are widely used in the petroleum industry, permit measurement of only fluid viscosity in shear flow. In addition, the torque transducers in the Fann instruments are less sophisticated than those in the instruments listed above. The rheometers which we have used in this research are the Rheometrics System IV Rheometer and the Rheometrics Pressure Rheometer. In my opinion the Rheometrics Pressure Rheometer is the best general purpose instrument for characterizing fracturing fluid gels. For research on chemical kinetics using dynamic oscillatory measurements the greater sensitivity of the Rheometrics Fluids Rheometer is desirable, but this instrument does not permit measurment of gel properties above the boiling point of water. My evaluation of the existing instrumentation is as follows:

Contraves: The Contraves is noted for its ability to measure very small torque signals in steady shear. This is not a key requirement for gels. The instrument has a very limited ability to perform dynamic measurements. The sample geometry is fixed and it would be impossible to use this instrument with on-line injection of the the gel.

Haake CV 100: This instrument has the capability to measure small torque signals and to perform dynamic measurements over a limited range of frequencies. It is rugged and easy to use. The lower cup on this instrument, which is driven by the motor, is inaccessible and it would not be possible to use this instrument with on-line injection.

Weissenberg-Sungamo Rheogoniometer: This instrument performs steady shear, dynamic oscillatory shear, and dynamic oscillatory shear superimposed on steady shear. The latter measurement might be of some value in investigating gel properties. The instrument has a readily accessible sample chamber and it would be easy to investigate different sample geometries. It would be possible to perform on-line injection. Temperature control is provided by an air oven and this is less precise and slower in response time than the fluids bath on the Rheometrics or Haake instruments. The instrument has the reputation for taking much more care and time to align and operate than the Rheometrics or Haake instruments. Therefore the instrument would be less productive in terms of information and samples processed per day than the Rheometrics or Haake instruments. The sophistication of the electronics, control, and data acquisition are below that of the Rheometrics instruments.

Rheometrics System IV/ Rheometrics Fluids Rheometer: These two Rheometrics instruments share the same transducers and drive motors and ,therefore, perform equally well for fracturing fluid gels. The System IV has several other transducers and motors in the same instrument that make it suitable for characterizing polymer melts and solids. The instruments have circulating fluid temperature baths that allow regulation between -20°C and 80°C. The sample chamber is accessible and permits the user to experiment with alternate test geometries. Shear rate ranges from 0.001 to 10,000 s^{-1} and frequency ranges from 0.01 to 100 rad/s are possible. However, most often measurements on gels are limited by the torque sensitivity of the transducer. The 100 g-cm transducer allows for steady shear measurement and dynamic measurements of gels, but large strains (e.g. 100%) must be used at low frequencies (e.g., 10 rad/s) to obtain measurable torque signals. The more sensitive 10 g-cm transducer is better suited for measuring the dynamic properties of gels since smaller strains can be imposed. However, in steady shear the torque capacity of the 10 g-cm transducer is exceeded at about 100 s^{-1} with the standard parallel plate geometry. With the optional micro-computer data acquisition system it is possible to do shear rate tests to mimic shear histories during fracturing fluid injection. It also permits the storage of data on floppy disks, so that data from different experiments can be superimposed, which we consider a major advantage.

Rheometrics Pressure Rheometer: This is the only commercially available instrument that performs steady shear and dynamic oscillatory measurements at elevated pressures so that measurements of gel properties above the boiling point of water are possible. Measurements to over 250°C and several hundred psi are possible. The instrument specifications are similar to those of the Fluids Rheometer with the 100 g-cm transducer. However, the upper frequency range is slightly reduced because of the greater inertia of the Couette fixture in the Pressure Rheometer, and the torque sensitivity is not quite as good as the Fluids Rheometer. The decreased torque sensitivity (compared to the 100 g-cm Fluids transducer) makes it difficult to perform some dynamic oscillatory measurements on weak gels. With some "re-plumbing" it is possible to inject gels into the sample chamber through the air line used to pressurize the system. This arrangement is, however, awkward. Compared to the Fann 50 viscometer, the Rheometrics Pressure Rheometer is more sensitive and more accurate, has modern data acquisition and display, and allows dynamic oscillatory measurements.

ACKNOWLEDGMENTS

We wish to acknowledge the financial assistance provided by the American Petroleum Institute. The work was conducted by Alice Chu, a post-doctoral research associate, and Jeffrey Kramer, a doctoral student at Princeton University. Special thanks go to Dr. Ralph Veatch, PRAC Committee Chairman, for his encouragement and direction in administrative and technical matters, and to Dr. John Cameron, PRAC Committee Vice-Chairman, for his careful critique of experiments and drafts of this final report. Dr. Cameron's contribution in finding the error in the original wall slip calculations (Appendix A) is acknowledged. Also, I want to thank the PRAC Committee members for their patience in teaching a rheologist about the art, science, and mystery of hydraulic fracturing.

REFERENCES

1. K. te Jigen Nuis, Colloid Polymer Science, 259, 522 (1981).

2. J. D. Ferry, Adv. Protein Chem., 4, 1 (1948).

3. R. Roscoe, Rheologica Acta, 19, 737 (1980).

4. J. T. Uhl, R. K. Prud'homme, Macromolecules (submitted).

5. R. K. Prud'homme, J. T. Uhl, J. P. Poinsatte, and F. Halverson, Soc. Pet. Engrs. J., 804-808, Oct. 1983.

6. J. D. Ferry, Viscoelastic Properties of Polymers, 3rd ed., John Wiley and Sons, NY, 1980.

7. D. S. Pearson and W. W. Graessley, Macromolecules, 13, 1001, (1980).

8. Personal communication from Dr. William Stivers, Celanese Chemical Co., Jeffersontown, KY.

9. Personal communication from Dr. Donald Putzig, du Pont Inc., Jackson Laboratory, Deepwater, NJ.

10. Personal communication from Dr. James Steinmutz, Kay-Fries, Inc., Stony Point, NY.

11. G. Rummo, Oil and Gas J., Sep. 13, 84 (1982).

12. P. Kolodziej, C. W. Macosko, and W. E. Ranz, Polym. Eng. and Sci., 22, 388 (1982).

13. C. Tucker, III, and N. P. Suh, Polym. Eng. and Sci., 20, 875 (1980).

14. R. B. Bird and P. J. Carreau, Chem. Engr. Sci., 23, 427-434 (1968).

15. R. B. Bird, O. Hassager, R. C. Armstrong and C. F. Curtiss, Dynamics of Polymeric Liquids, Vol. 2, John Wiley: New York (1977), Ch.15.

16. P. J. Carreau, Trans. Soc. Rheol., 16, 99-127 (1972).

17. A. Kaye, Brit. J. Apl. Phys., 17, 803-806 (1966).

18. A. S. Lodge, Rheol. Acta., 7, 379-392 (1968).

19. R. I. Tanner and J. M. Simmons, Chem. Engr. Sci., 22, 1803-1815 (1967).

APPENDIX A

WALL SLIP CORRECTIONS FOR THE COAXIAL CYLINDER VISCOMETER

by

Ann S. Yoshimura
Robert K. Prud'homme

Department of Chemical Engineering
Princeton University
Princeton, New Jersey 08544

Rheological measurements on gels, concentrated suspensions, and foams are often confounded by slip at solid boundaries with the result that the flow field, or kinematics, is unknown. To interpret experimental data it is necessary to correct for slip at boundaries. In this note we present the analysis of Couette flow between coaxial cylinders with wall slip. From experiments on two Couette geometries we show how to calculate the total wall slip velocity, and, for the case of small gaps, the fluid viscosity.

The coaxial Couette geometry to be considered is shown in Fig. 1. The bob is held stationary, the cup is rotated at angular velocity Ω, and the torque T on the bob is measured. A list of nomenclature and symbols can be found at the end of the text.

It can be shown from the θ-equation of motion that the shear stress is given by

$$\tau_{r\theta} = \frac{T}{2\pi L r^2} \quad . \qquad (1)$$

The rate of strain in a cylindrical coordinate system is defined by

$$\dot{\gamma}_{r\theta} = r \frac{d}{dr} \left(\frac{v_\theta}{r} \right) \quad . \qquad (2)$$

For a fluid at steady state the rate of strain is a unique function of the imposed stress; therefore Eqn. 2 can be written

$$r \frac{d}{dr} \left(\frac{v_\theta}{r} \right) = f(\tau_{r\theta}) \quad . \qquad (3)$$

Eqn. 1 can be used to change independent variables in Eqn. 2 from r to $\tau_{r\theta}$,

$$\frac{d}{d\tau_{r\theta}} \left(\frac{v_\theta}{r} \right) = - \frac{f(\tau_{r\theta})}{2\tau_{r\theta}} \quad , \qquad (4)$$

which can then be integrated from the bob ($r = R$) to the cup ($r = \kappa R$) to yield

$$\left.\frac{v_\theta}{r}\right|_{r = \kappa R} - \left.\frac{v_\theta}{r}\right|_{r = R} = \int_{\tau_c}^{\tau_b} \frac{f(\tau_{r\theta})}{2\tau_{r\theta}} \, d\tau_{r\theta} \quad . \qquad (5)$$

The slip velocities S_b and S_c are defined as the difference between the velocity of the solid wall and the fluid velocity at the wall;

$$S_b = v_\theta \big|_{r = R} \quad , \qquad (6)$$

$$S_c = \Omega \cdot \kappa R - v_\theta \big|_{r = \kappa R} \quad , \qquad (7)$$

and are assumed to depend only on the wall shear stresses τ_b and τ_c. It should be noted that the slip velocities at the cup and bob surfaces are not equal since, as can be seen from Eqn. (1), the stresses are not equal. Combining these expressions with Eqn. (5) yields

$$\Omega = \frac{1}{R}\left[S_b(\tau_b) + \frac{S_c(\tau_c)}{\kappa}\right] + \int_{\tau_c}^{\tau_b} \frac{f(\tau_{r\theta})}{2\tau_{r\theta}}\, d\tau_{r\theta} \quad . \qquad (8)$$

The first term on the right in brackets represents the slip contribution to the angular velocity Ω, while the integral term accounts for deformation of the liquid.

The slip velocities and true rate of strain in the fluid can be determined from experimental data in the following manner.

A. <u>Calculation of Slip Velocities</u>

The slip term can be evaluated by using two Couette tools of different R but with the same κ. For bobs of radii R_1 and R_2, and of lengths L_1 and L_2, if the torques are chosen such that

$$\frac{T_1}{T_2} = \frac{L_1 R_1^2}{L_2 R_2^2} \quad , \qquad (9)$$

then the same shear stress will be produced on each bob. From Eqn. (1),

$$\frac{\tau_c}{\tau_b} = \frac{1}{\kappa^2} \quad . \qquad (10)$$

Since κ is the same for both devices, the shear stresses at the cups are also equal.

Applying Eqn. (8) to each device gives

$$\Omega_1 = \frac{1}{R_1}\left[S_{b1}(\tau_{b1}) + \frac{S_{c1}(\tau_{c1})}{\kappa}\right] + \int_{\tau_{c1}}^{\tau_{b1}} \frac{f(\tau_{r\theta})}{2\tau_{r\theta}}d\tau_{r\theta} \quad , \tag{11}$$

$$\Omega_2 = \frac{1}{R_2}\left[S_{b2}(\tau_{b2}) + \frac{S_{c2}(\tau_{c2})}{\kappa}\right] + \int_{\tau_{c2}}^{\tau_{b2}} \frac{f(\tau_{r\theta})}{2\tau_{r\theta}}d\tau_{r\theta} \quad . \tag{12}$$

Since

$$\begin{aligned} \tau_{b1} &= \tau_{b2} \quad , \quad \text{and} \\ \tau_{c1} &= \tau_{c2} \quad , \end{aligned} \tag{13}$$

it follows that

$$\begin{aligned} S_{b1} &= S_{b2} \quad , \quad \text{and} \\ S_{c1} &= S_{c2} \quad . \end{aligned} \tag{14}$$

Therefore, Eqns. (11) and (12) can be subtracted to yield

$$\left[S_b(\tau_b) + \frac{S_c(\tau_c)}{\kappa}\right] = \frac{\Omega_1 - \Omega_2}{1/R_1 - 1/R_2} \quad . \tag{15}$$

From Eqn. (15) the total slip velocity can be calculated. This expression can then be inserted into either Eqn. (11) or (12) to give the actual (corrected) angular velocity experienced by the liquid,

$$\Omega_{corrected} \equiv \int_{\tau_c}^{\tau_b} \frac{f(\tau_{r\theta})}{2\tau_{r\theta}} \, d\tau_{r\theta} = \frac{R_2\Omega_2 - R_1\Omega_1}{R_2 - R_1} \quad . \tag{16}$$

B. Calculation of Fluid Viscosity

The determination of the corrected angular velocity from measurements with two sets of geometrically similar Couette coaxial cylindaers (i.e., Eq. 16) is a new result. The derivation makes no assumption about whether the gap between the cylinders is "narrow" (i.e., $\kappa \sim 1$) or "wide" (i.e., $\kappa > 1$). The calculation of fluid viscosity, however, from measured torque and corrected angular velocity is accomplished conveniently only when either "narrow" or "wide" gap approximations can be made (1). For the case of "wide" gaps Krieger (2) has resented a series solution that converges rapidly.

Most Couette viscometers are designed so that the "narrow" gap approximation is valid. For a difference in radii between the cup and the bob of 5%, the stress across the gap will deviate from its mean value by ± 5%. If this level of accuracy is acceptable, then the stress can be considered approximately constant across the gap, and the viscosity and rate of strain can be calculated from (3,1):

$$\eta \doteq \frac{(\kappa^2 - 1)T}{4\pi L\kappa^2 R^2 \Omega_{\text{corrected}}} , \qquad (20)$$

$$\dot{\gamma}_{r\theta} \doteq \frac{\kappa\Omega_{\text{corrected}}}{(\kappa - 1)} . \qquad (21)$$

References

1. Schowalter, W. R., Mechanics of Non-Newtonian Fluids, Pergamon Press, NY, 1978, pp. 94-96.

2. Krieger, I. M., Trans. Soc. Rheol, 12, 5 (1968).

3. Bird, R. B., W. E. Stewart, and E. N. Lightfoot, Transport Phenomena, John Wiley and Sons, NY, 1960, p. 95.

Notation

r, θ	radial, tangential coordinates respectively
v_θ	tangential fluid velocity $[\ell/t]$
S_b	slip velocity at bob $[\ell/t]$
S_c	slip velocity at cup $[\ell/t]$
Ω	angular velocity of cup $[t^{-1}]$
T	torque on bob $[F \cdot \ell]$
$\tau_{r\theta}$	$r\theta$-component of the stress tensor (shear stress) $[F/\ell^2]$
τ_b	shear stress at bob
τ_c	shear stress at cup
γ	rate of strain $[t^{-1}]$
R	bob radius $[\ell]$
κ	ratio of cup radius to bob radius
L	length of bob $[\ell]$

APPENDIX B

An impingement mixing device was constructed to mix guar and titanate solutions since mixing in a blender produced gels with inconsistent properties. The concept for the mixing device comes from impingement mixers used in reaction injection molding of polyurethane. A schematic of the mixer is attached and a parts list is included. Mixing occurs as the guar and titanate solutions impinge on each other in a three-way tee fitting, and further mixing occurs as the mixed solution flows through a 3" section of 1/4" OD stainless steel tubing filled with 24-32 mesh (0.71 - 0.50 mm) sand. The guar and titanate are loaded into a double-acting, stainless steel hydraulic cylinder and microliter syringe, respectively, by positioning a six-port chromatography valve so that solutions can be drawn into the cylinder and syringe. Fluid is sucked into the guar cylinder but is injected into the titanate syringe using a larger 10 ml syringe as the titanate "reservoir" shown in the figure. The piston rod of the double acting hydraulic cylinder is mechanically coupled to a rod that drives the microliter syringe plunger. The cross-sections of the cylinder (17/16") and syringe (250 microliter volume) determine the ratio of guar to titanate solutions.

After loading, the 6-port valve is rotated to the "inject" position. Mixing begins when an on/off valve is opened to pressurize the back of the double acting cylinder with 200 psi nitrogen. The first few milliliters of mixed gel are discarded by directing the flow to a waste vessel using a three-position valve, and then the flow is directed into the stem of a special cup we have constructed for our System IV Rheometer.

After an injection, the lines and sand-pack are flushed with HCl solution, DI water, and then methanol to remove residual gel. Nitrogen gas is used to dry the lines and sand-pack before the next injection.

Parts List

1. Bimba double acting, stainless-steel cylinder Model D4173A-6 (Bimba Manufacturing, Monee, IL). This cylinder may be disassembled for cleaning.
2. Hamilton 250 microliter Gas-Tight Syringe, Cat. No. 1725-TEFLL (Hamilton Inc., Reno, NV).
3. Becton-Dickinson three-way screw-type stopcock (Becton-Dickinson, Inc., Rutherford, NJ.)
4. Teflon chromatography tubing: 1/8" OD x 2.4 mm ID, Cat. No. 3134; 1/16" OD x 1.0 mm ID, Cat. No. 3132 (Alltech, Deerfield, IL).
5. Alltech plastic liquid chromatography fittings.
6. Six-port valve similar to Valco (Valco Instruments Co., Houston, TX).

FIG. B1

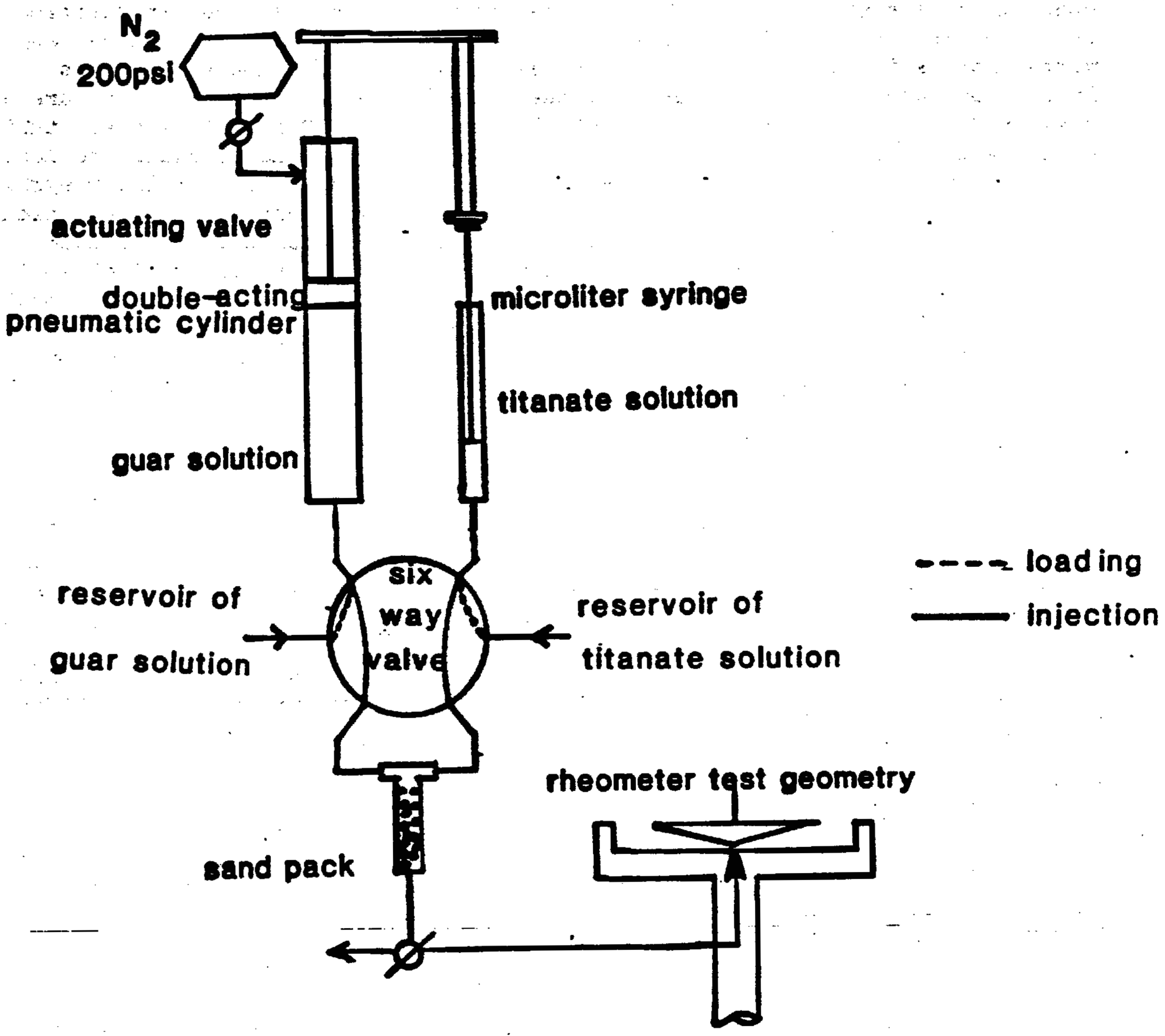

Impingement mixing device

FIG. B2

RKP
6/84

IMPINGEMENT MIXER

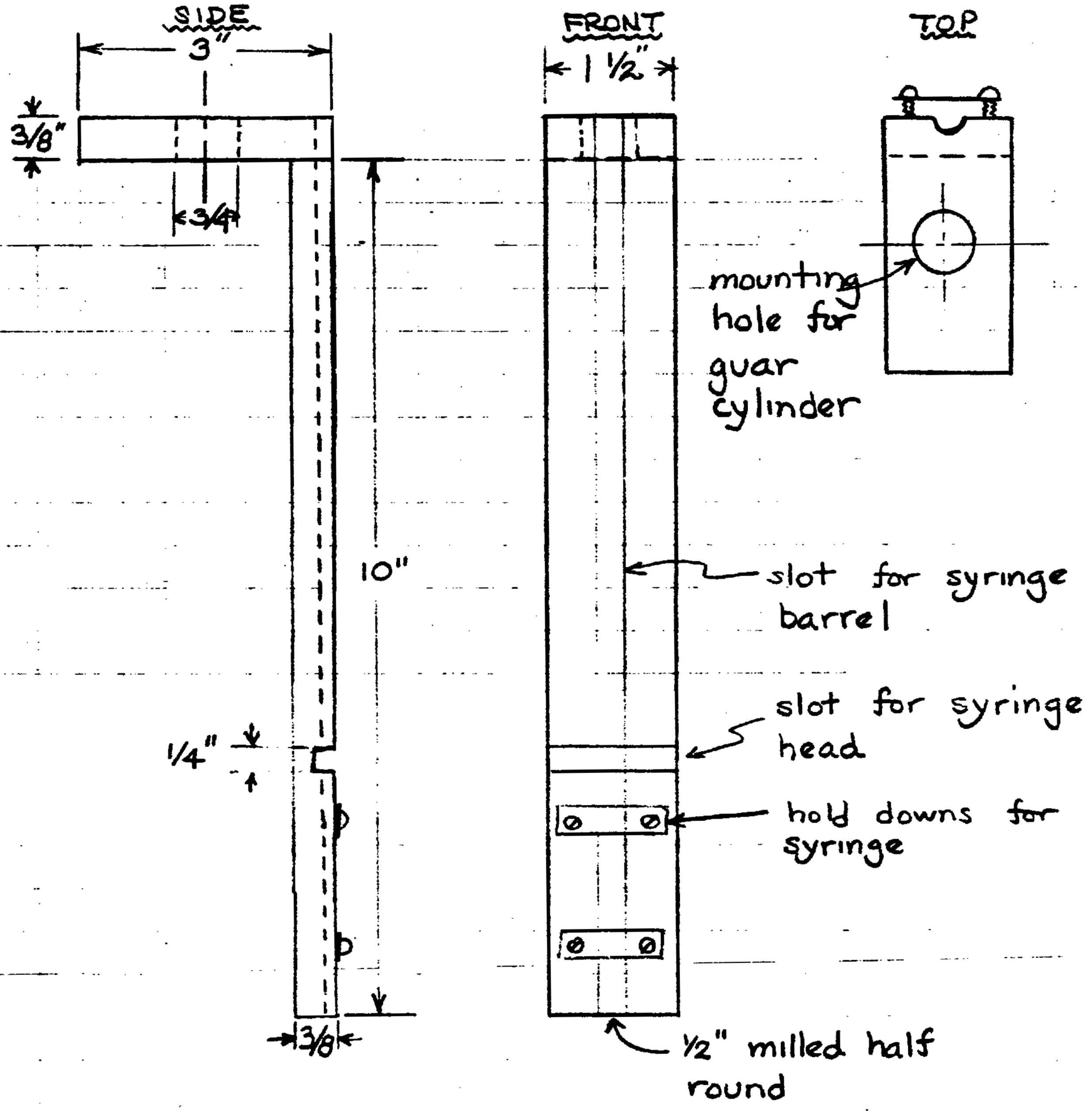

PLUNGER LINKAGE:

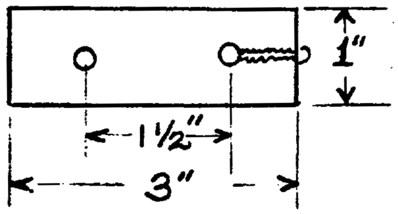

hole threaded for cylinder plunger
1/4" hole for driving rod,
w/ set screw

MIXING TEE:

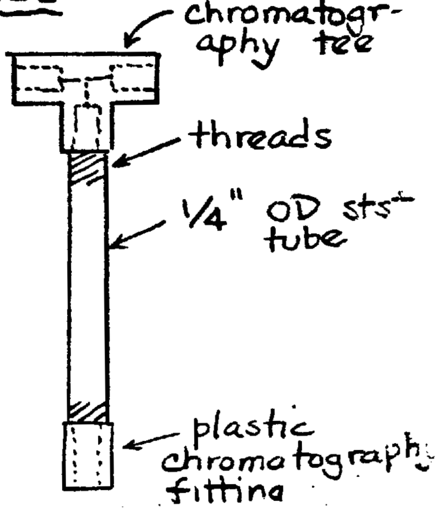

APPENDIX C

Continuous Shear Flow Apparatus

Theory of Operation

The schematic of the capillary viscometer showing the reversal of flow direction is shown in Fig. C.1. The guar solution and cross-linking agent are mixed and injected into the flow system by a mixing device described in Appendix B. Non-reactive driving fluid is supplied from a high pressure liquid reservoir located at the top of the system. The direction of flow is controlled by three pneumatically driven computer-controlled valves. The valves are switched, and the direction of flow reversed when a specified amount of driving fluid has been collected in the electronic balance apparatus. The balance interfaces with the computer through an RS-232 link. The amount of driving fluid collected is chosen so that the crosslinked gel is kept in the center testing section and under steady shear conditions. Capillary pressure drops are determined by three pressure transducers and are recorded by the computing system through an A/D converter.

Specifications

ID tubing: 1/32"

Capillary Length (Middle testing section): 910 cm

Driving Pressure: 200 psi

Shear Rate at Wall: 1500 s^{-1}

Fluid Flow Rate: 0.0737 cm/s

Pressure Transducers: Celesco Model P7D

Valves Switching Time: approx. 15 ms.

Computing System: IBM PC

CONTINUOUS SHEAR FLOW APPARATUS

FIG. C1

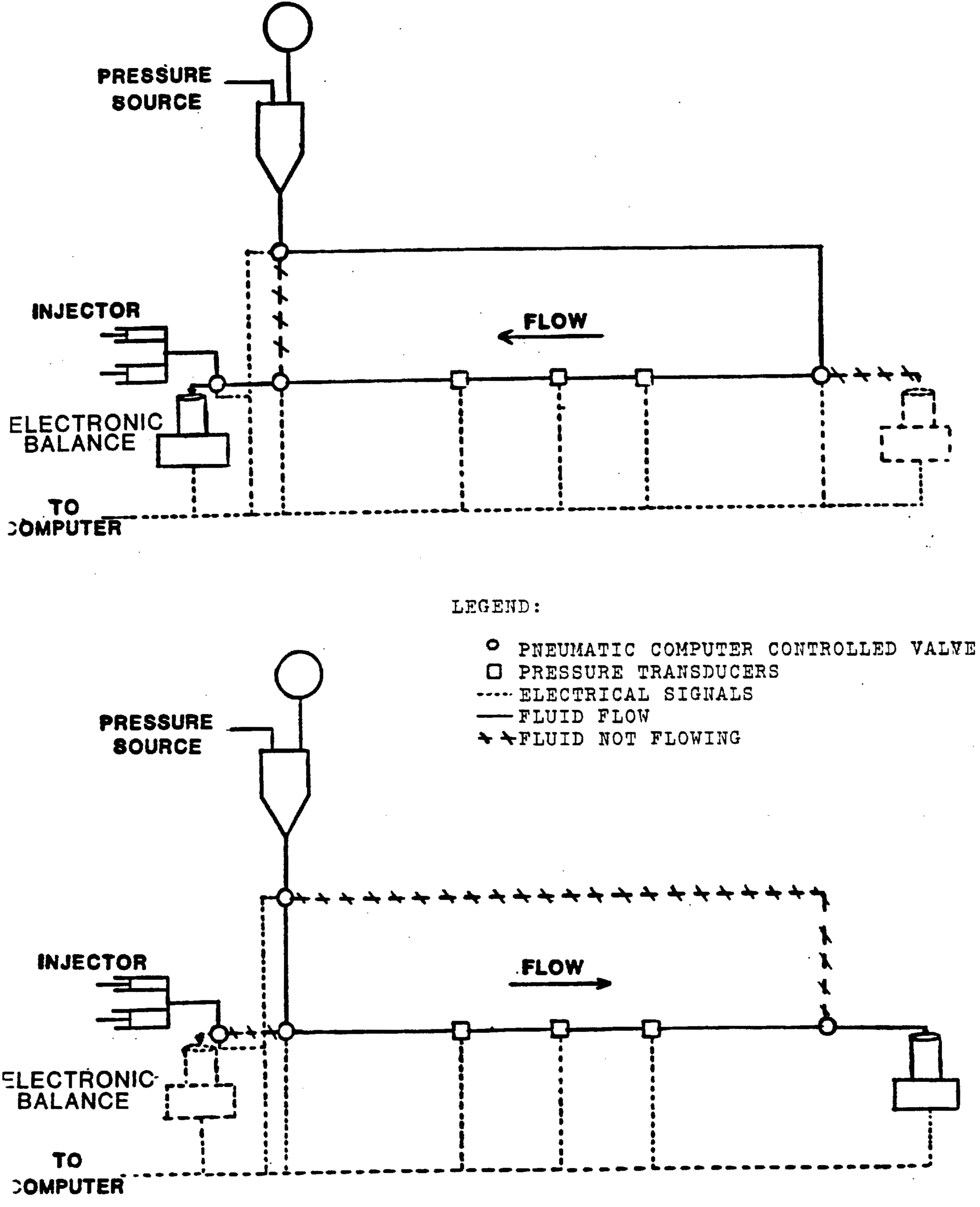

LEGEND:

- ○ PNEUMATIC COMPUTER CONTROLLED VALVE
- □ PRESSURE TRANSDUCERS
- ------ ELECTRICAL SIGNALS
- —— FLUID FLOW
- ✕✕ FLUID NOT FLOWING

APPENDIX D

Prepared by Dr. John Cameron
PRAC Committee Vice- Chairman, 7 Dec. 83

Outline Summary of PRAC Project 82-45 Research During 1983

I. Measurement of Viscous and Elastic Properties at Low Shear Rates
  A. Hydration and Structure of Guar solutions @ 25 C using the Systems IV Mechanical Spectrometer
    1. steady shear sweeps (2/28/83)
    2. strain sweeps (2/28/83)
    3. frequency sweeps (2/28/83)
    4. effect of mixing sequence via G' from strain and frequency sweeps (6/12/83)
    5. effect of isopropanol via G' from strain and frequency sweeps (6/12/83)

  B. Properties and structure of 0.4% Tyzor TE gel @ 25 C using the Systems IV Mechanical Spectrometer (2/28/83)
    1. strain sweep
    2. frequency sweep
    3. temperature sweep from 25 to 100 C
    4. gelation time @ 25 C
    5. step shear rate (1, 10, 100, and 1 1/s)

  C. Properties and structure of .04% Tyzor AA gel @ 27 C using the Systems IV Mechanical Spectrometer or the Rheometrics Pressure Rheometer (RPR)
    1. gelation time @ 27 C via G' by varying guar and Tyzor AA concentration (6/12/83 -- Systems IV)
    2. effect of mixing sequence via G' from strain and frequency sweeps (6/12/83) and (9/5/83 -- Systems IV)
    3. effect of Tyzor AA aging via G' from dynamic time sweep (6/12/83 -- Systems IV)
    4. effect of diketone via G' from dynamic time sweep at various diketone concentrations (6/12/83 -- Systems IV)
    5. effects of shear via G' from alternating steady shear and oscillatory testing (6/12/83 -- RPR) and (9/5/83 -- Systems IV)
    6. Equilibrium viscosity tests via steady shear tests using fresh samples at each shear rate; two cone angles used (9/5/83 -- Systems IV)
    7. Viscosity of guar solutions at high shear rates using parallel plate geometry (procedure using rotational viscometer being written up) (9/5/83 -- Systems IV ?) (results of this work has not yet been presented to the API TAC)

  D. Construction of a pneumatic syringe for the continuous injection of guar and cross-linker during rheometer loading (9/5/83)

II. Slip Flow Studies

A. Cone-and plate wall slip and inertial effects testing using Brookfield standard solution 1000 and mineral oil @ 25 C; two cone angles used (9/5/83 -- Systems IV)

B. Equilibrium viscosity tests @ 25 C via steady shear tests using fresh samples at each shear rate; two cone angles used (9/5/83 -- Systems IV)

C. Construction of new Couette tools for measuring wall slip (9/5/83 -- Systems IV)

D. Derivations of equations for analysis of Couette flow with slip (assuming slip velocity to be a function of wall shear stress) (9/5/83)

III. Gel Rheology at High Shear Rates

A. Ordering of hardware for reciprocating capillary viscometer (computer received and functioning)

IV. Kinetic Modeling

A. Modification of existing polymer network theory models to incorporate chemical reaction kinetics (9/5/83) (Results of this work has not yet been reported to the API TAC)

V. Projected PRAC Project 82-45 Research for Balance of 1983

A. Use of Couette geometry to quantify slip

B. Continuation of dynamic testing immediately following steady shear testing to show effects of steady shear on gel viscoelasticity

C. Continuation of model development for gel cross-linking

D. Development of reciprocating capillary viscometer for time at temperature studies (slip and high shear studies too?) $5000\ s^{-1}$

E. Rheological testing of gels at high temperature and pressure (Systems IV or RPR)

JRC
83340ART0246